NEAR INFRARED SPECTRAL REFLECTANCE OF SIMULATED MARTIAN FROSTS

Thesis by
Hugh H. Kieffer

Submitted May 14, 1968

In Partial Fulfillment of the Requirements
For the Degree of
Doctor of Philosophy

California Institute of Technology
Pasadena, California
1968

ACKNOWLEDGEMENTS

I wish to thank Dr. Andrew Ingersoll, Dr. Bruce Murray, and Dr. Barclay Kamb for their continued interest and suggestions during this work. The many technical discussions with each of this triumvirate were a valuable contribution to this work. The willingness of Mr. James Westphal to spread his knowledge of electronics and infrared instrumentation was a great help throughout the experimental work. Dr. Gary Neugebauer kindly loaned me the variable interference filter though it meant continued inconvenience to him. Messrs. Sol Giles and Curtis Baumen were of considerable assistance with the mechanical and vacumn apparatus. Messrs. Victor Nenow and Devere Smith often came to my aid when electronics problems were encountered.

I owe much to my wife Susan, whose ability and willingness to run a secretarial service, a home, maintain good spirits and continue her own studies during the production of this thesis were especially appreciated.

The author was supported by a National Aeronautic and Space Adminstration Traineeship during part of this investigation. Much of the research expense was supported by NASA Grant 56-60.

ABSTRACT

In view of the apparent conflict between spectral observations and recent theories of the Martian polar caps, comparison spectra were obtained for frosts of relevant composition and grain size. The spectral reflectances of frosts formed from pure CO_2, and pure H_2O and mixtures of these gases have been measured from 0.8 to 3.2 μ. Low-weight fractions or small surface concentrations of H_2O resulted in spectra similar to pure H_2O frost spectra. The concentration of the condensible gas and the radiation balance effect the frost textural scale and the contrast of the reflection spectrum. The emissivity of the polar caps may be small, in contrast to previous assumptions. Probable processes of frost formation and sublimation on Mars and seasonal variations of frost composition suggest that reflection spectra obtained in the Martian spring may be misleading. In light of the laboratory results and probable Martian conditions, previous suggestions that the Martian polar caps are H_2O are not valid. Future diagnostic observations in the near and thermal infrared are suggested.

Figures 10, 11 and 12 are photographs of frost samples and will not reproduce well. Photographic copies may be ordered.

TABLE OF CONTENTS

page

I. INTRODUCTION

A. Basis, aim and scope of this thesis 1

B. Relevant facts about Mars 3

C. The problem of observing Martian polar caps 4

D. Observations of the Martian polar caps 5

E. Theories of the Martian polar caps 6

II. LABORATORY MEASUREMENTS

A. Introduction 8

B. Apparatus and method 9

C. Reference and substrate reflectance 10

D. Gas and liquid transmission spectra 11

E. CO_2 frost reflection spectra 12

F. H_2O frost reflection spectra 13

G. CO_2-H_2O mixed frost reflection spectra 15

H. Summary of laboratory spectral measurements 17

III. FROST TEXTURE AND SPECTRAL PROPERTIES

A. Introduction 18

B. Variations in texture

1. Dependence of texture on relative concentration 20

2. The effect of radiation cooling versus substrate cooling on texture 21

3. Metamorphism and sublimation 22

C. Variations in spectral properties

1. Dependence of spectral reflectance on grain size 23

2. Angular dependence 23

D. Summary: The composition, texture and reflectance of Martian frosts 24

1. CO_2 polar caps 25

2. H_2O polar caps 26

IV. CONCLUSIONS

A. Introduction 28

B. Interpretation of existing Martian polar cap spectra 29

C. Future observations 30

D. Thermal flux as a diagnostic test 32

Figures and Figure Captions 33

APPENDICES

I. INSTRUMENTATION 51

II. DETAILED PROCEDURE 61

III. FROST EMISSIVITY AND RADIATION BALANCE OVER THE MARTIAN POLAR CAP 67

IV. SPECTRAL AND PHYSICAL PROPERTIES OF H_2O AND CO_2 73

V. ORIGINAL STATEMENTS OF KUIPER, MOROZ AND DOLLFUS 77

Appendix Figures and Captions 83

Appendix Tables 88

References 91

I. INTRODUCTION

Basis, Aim and Scope of this thesis

For nearly twenty years, infrared spectral (Kuiper, 1952, pp. 361-362; Moroz, 1964, p. 279) and visual polarization (Dollfus, 1961, pp. 381-382) observations of the Martian polar caps have been interpreted to mean that the caps are composed of H_2O frost. Theoretical discussions (Leighton and Murray, 1966) based on recent determinations of the composition and pressure of the Martian atmosphere suggest that H_2O caps would require an extreme planetary circulation system whereas a model of CO_2 frost caps does not require exceptional meteorology and is compatible with all information about Mars except the interpretation of the cap spectra. Existing information has been insufficient to resolve this discrepancy. There has been a lack both of observational data and of adequate comparison spectra.

The information needed first was comparison spectra covering the range of frost types likely on Mars. This would allow both a more critical interpretation of the existing observations and the optimum design of future Martian observational experiments.

This basic purpose of this thesis is to provide these comparison spectra, that is, to measure the reflection spectra of frosts with sufficient range in composition and physical characteristics to cover the probable frost types on Mars. Polarization measurements were not made as polarization is more dependent on texture than is spectral reflectance (see, for instance, the laboratory measurements by Dollfus, 1961, pp. 350-366). It is not likely that polarization measurements would yield diagnostic results as to composition under any circumstances.

The relevant observations of the Martian atmosphere and polar caps are discussed in this introduction. From these observations and simple theoretical considerations, it is shown that the only likely candidates for the Martian caps are H_2O and CO_2.

The spectral reflectances of H_2O - CO_2 frosts measured in the lab are presented in Section II. The near infrared was studied as H_2O and CO_2 frosts are both white in visible light and thermal emission becomes a significant problem beyond 5μ. It was apparent early in the experimental work that the addition of small amounts of water made appreciable changes in the CO_2 spectra but not vice versa, and consequently, the low water concentration range was studied most extensively. Low angle back-scatter reflectance, simulating Earth-Mars opposition geometry, was measured for some frosts and indicated that the laboratory measurements at normal incidence and reflection were applicable to Martian observations. The laboratory apparatus and procedure are discussed briefly in Section II and in more detail in Appendixes I and II.

Most of the frosts grown in the laboratory were fine-grained and variations in spectral reflectance with increasing grain size were observed. "Grain size" here means the scale of the grain texture effecting scattering (volume to surface ratio), not mean grain diameter. The validity of relating the laboratory results to Martian frosts is discussed in Section III, where the variations of frost texture with environment and the resulting changes in spectral properties are treated. These useful and necessary concepts previously have been largely ignored in discussions of the Martian polar caps. While the behavior and form of H_2O frosts on Mars would be much the same as on Earth, the condensation of CO_2 on Mars has no terrestrial analogy. It is shown that the process of CO_2 freezing on Mars may be impossible to duplicate exactly in a laboratory, or in fact, on less

than a planetary scale. The emissivity of CO_2 frosts may not be near unity, as has previously been assumed. The relations between Martian CO_2 frost texture, radiation balance, and cloud formation and composition are discussed in Appendix III. Section III concludes with a discussion of the probable frost forms and apparent composition for both H_2O and CO_2 models of the Martian polar caps. Much of the material in this section is necessarily qualitative as in most cases quantitative theories are altogether lacking.

Finally, the laboratory results and theoretical discussions are applied to the interpretation of the existing observations and to the definition of future observations (Section IV) . It is shown that the existing observations of the polar cap are inconclusive and do not demonstrate that the Martian caps are composed primarily of H_2O.

Relevant facts about Mars

Recent determinations of the amount of CO_2 in the Martian atmosphere have ranged from 55 ± 20 to 90 ± 27 meter-atm., with perhaps the most reliable value being near 90 meter-atm. (Spinrad et al., 1967, p. 336) . This is equivalent to a surface partial pressure of 6.6 mb. Spectroscopic determinations of the total surface pressure range around 10 mb, and the Mariner IV occultation experiment data suggest a surface pressure of 5 to 6 mb. It appears likely that much, or nearly all, of the Martian atmosphere is composed of CO_2.

The only other gas positively identified in the Martian atmosphere is H_2O. The recent work of Schorn et al. (1967) indicates its abundance to be 10 to 20 precipitable microns. They found evidence that the water vapor abundance is correlated in time and location with the growth and recession of the polar caps. The observed water vapor concentrations suggest to them that the average temper-

ature of the lowest one-half (by mass) of the atmosphere cannot be much less than 200°K (p. 750).

The nitrogen oxides had been proposed as major components of the Martian atmosphere (Kiess, et al., 1960); however, very low upper limits on their concentrations have been placed. Marshall (1964) set an upper limit of 8 micron-atm. on the amount of NO_2 in the Mars atmosphere. This limit has been confirmed by Owen (1966).

Kaplan, Münch and Spinrad (1964) have placed an upper limit on O_2 of 70 cm-atm. Upper limits on the concentrations of several gases have been placed on the basis of there being no observable absorption effect in the Martian spectra. These values are summarized in Lippincott et al. (1967).

No reliable measurement of the temperature of the polar caps has been made. Such a measurement would be extremely important in the determination of their composition.

The problem of observing Martian polar caps

The polar caps of Mars are small and difficult to observe. Their apparent area comprises at most a few percent of the planetary disk. They are, of geometrical necessity, viewed obliquely. Historically, observations of Mars have been made primarily near the time of oppositions, i.e., when the earth is in the same direction from the planet as the sun. Therefore, the season of the dominant hemisphere is summer rather than winter. The apparent area of Mars varies by a factor of four between good and poor oppositions with the good oppositions occurring in the late Martian southern spring. Hence the observational geometry of the polar caps is always poor, particularly for the northern cap. Under the most favorable observational conditions, the polar caps subtend only about 2 x 5 seconds of arc,

as compared to typical astronomical seeing of about 2 seconds of arc. Observation of the formation of the polar caps is a most difficult problem and no spectra or polarization measurements have been made of this phase.

Observations of the Martian polar caps

The only infrared spectral observations of the Martian polar cap reported are those of Kuiper (1952) and Moroz (1964). Both men reduced the spectral resolution of their equipment to one-ninth the wavelength in order to have the sensitivity required to detect light reflected from the polar cap alone. The apparent sizes of the polar cap when Kuiper and Moroz made their measurements were about 2 and 1.5 (my calculation) square seconds of arc respectively. Their comments and data on the polar cap are quoted in full in Appendix 5.

Kuiper observed natural snows and water frost formed on dry ice and found the spectra to be equivalent to those of water absorption cells of different thickness. He makes no mention of the marked frequency shifts between H_2O gas, liquid and solid absorption features. He found terrestrial snow "nearly black beyond 1.5 microns and almost fully black beyond 2.0 microns". Measurements with CO_2 snow showed it to remain "white" up to 2.5 microns except for the 2 micron absorption band. The reflection spectrum of the Martian polar cap was similar to terrestrial snow "though the drop at 1.5 microns is less steep." No data or spectra of Martian caps, H_2O or CO_2 frosts were published. Kuiper does not state the date of his observations. He concludes that "the Martian polar caps are not composed of CO_2 and are almost certainly composed of H_2O frost at low temperature (much below 0° C)".

Moroz observed the polar cap spectrum in the region of 1 to 2 microns and compared it with the spectrum of the center of the planet. He states that, on the

average, the cap spectrum had a lower intensity in the 1.5 to 1.8 micron region than that of the central portion of the disk. He published averaged spectra of the cap and the center of the planet. His observations were made of the northern polar cap when it was in the late spring season. Moroz interpreted the polar cap spectrum as being similar to the spectra of snow and hoar frost which he had observed.

Visual polarization measurements of the polar cap were made by Dollfus (1961). He found that the polar cap showed small, variable polarization during the spring. Natural snow and hoar frost deposits showed strong positive polarization, but the polarization of laboratory water frost, subliming at low pressure under intense illumination, was small and variable, similar to the Martian results. The edges of the polar caps showed very strong negative polarization, which Dollfus could correlate only with clouds of ice crystals. He made no observations on CO_2 clouds or frosts. His results and interpretations are included in Appendix 5.

Theories of the Martian polar caps

The observational constraints allow only two cases of significant probability. The first is that carbon dioxide freezes at the polar caps. As CO_2 is a major fraction of the atmosphere, diffusion gradients will not significantly alter its partial pressure. Therefore, saturation of CO_2 sets a firm lower limit on the temperature at all places on the planet of 145 to 151° K (3 to 7 mb). The temperature would be constant over the polar cap. The vapor pressure of water in the polar region would be limited by its saturation pressure at this temperature, i.e., approximately 10^{-7} mb equivalent to 10^{-3} precipitable microns in the atmospheric column. Unless the lapse rate in the polar regions is positive, the water vapor concentration could never be greater than this over the polar caps. There is no

clear limit to the amount of water which could be present as suspended crystals (snow). The behavior of the polar cap recession and planetary pressure for this case have been treated extensively by Leighton and Murray (1966).

The second case is that of no CO_2 freezing, i.e., with the polar caps composed entirely of water frost. The saturation temperature corresponding to the observed water vapor abundance places a firm maximum temperature on the forming polar cap. Specifically, 10 precipitable microns of water vapor mixed uniformly through the atmosphere corresponds to a surface water vapor pressure of 9×10^{-4} mb and a saturation temperature of about 198° K. The temperature of the spring polar cap has no clear upper limit other than that the vapor pressure of the subliming deposit cannot be greater than the total pressure. This would occur at about 6° C.

Leighton and Murray find that the CO_2 frost cap model is in reasonable accord with visual observations of Mars. The extreme planetary circulation system required in a model of H_2O polar caps leads them to "doubt that water could be the dominant constituent of the Martian polar caps (p. 6)".

One earlier candidate for the polar frost, N_2O_4 (Kiess et al., 1960) can be ruled out indirectly on the basis of chemical equilibria. Lippincott et al. (1967) compute the concentration of N_2O_4 to be three times that of NO_2 under equilibrium conditions. Even if N_2O_4 is three times as abundant as the upper limit of NO_2 (8 micron-atm) its partial pressure would be 2×10^{-6} torr. The saturation temperature for this concentration is less than 125° K. As this is well below the minimum temperature in accord with 6 mb of CO_2, N_2O_4 cannot freeze on the Martian surface.

II. LABORATORY MEASUREMENTS

Introduction

An experimental program was undertaken to provide comparison spectra for observations of the Martian polar caps. This involved measuring the near infrared spectral reflectance of frosts composed of CO_2, H_2O and $CO_2 - H_2O$ mixtures. It was desirable that the measurements include samples covering a wide range of grain size and composition.

The difficulty inherent in observing frosts without altering them required specifically designed apparatus. In particular, the incident flux required for reflectance measurements with standard spectrometers is prohibitive. In order to determine the grain size, composition and density of the samples, it was necessary that visual and mechanical access to the samples be possible without significantly affecting its texture or introducing contamination. In addition, the absence of previous reliable experiments of this type made unforeseen difficulties likely and indicated that it would be prudent to keep the apparatus as simple and versatile as possible. The apparatus and procedures used for these measurements are described below in general terms. They are described in detail in Appendix I and II.

Most observations were made with an incidence angle of 0° and a reflected angle of 12° to 20°. The angle listed for the inclined measurements is the angle of incidence. The angle of reflectance was 12° less (in the same plane). The reflectance spectra were obtained by comparing the intensity of light reflected by the frosts with that reflected by a calibrated reference surface. Long-period variations in gain and uncertainty in repositioning the reference surface resulted in some uncertainty of the absolute level of reflectance. Most of the spectra presented have been normalized to unity at 1.76 microns so that spectral contrast,

rather than reflectance, is emphasized. Neither CO_2 nor fine H_2O frosts have appreciable absorptance at this wavelength, so that the scale change due to this normalization is small. The data below 1.5 microns were not reliable for some of the early results and have been deleted from the corresponding spectra. The spectral data are shown in Figures 1 through 9. Textures typical of the laboratory frosts are shown in Figures 10 through 12.

Apparatus and method

The spectrometer and electronics were designed to minimize the incident flux required to obtain a good signal-to-noise ratio and employed three variations from common techniques: (Fig. 1, Appendix I)

1. Illumination of the sample with chopped, monochromatic light rather than blackbody radiation removed all but about 0.5% of the source energy and placed the signal reduction inherent in spectrometers before, rather than after, the sample.

2. Use of synchronous detection techniques made observations possible at very low signal levels.

3. Placement of the detector inside the sample chamber eliminated additional optical elements.

The principal part of the apparatus was the lid of the environmental chamber to which all the other parts were attached and through which all observations of the sample occurred. This allowed the use of very simple, readily interchangeable chambers.

The pressure and gas flow in the chamber was controlled by an elaborate system of valves, manometers and thermocouple gauges. Usually a non-condensible

buffer gas (nitrogen or helium, typically 3 torr) was let into the chamber before frost growth started to control the uniformity and grain size of the deposit.

The chambers were usually cooled by immersion in liquid nitrogen, which kept the immersed surface at 77° K. A few samples were grown with the chamber cooled to 140 to 180° K by immersion in cooled trichlorofluoromethane or n-propyl alcohol.

Spectral reflectances were measured from 0.8 to 1.65 microns with a set of eighteen discrete interference filters, and from 1.58 to 3.2 microns with a continuously variable interference filter. The reflectance of a reference surface was measured before or after each scan of a frost specimen. These data were digitized and punched on paper tape for later processing by a computer.

The response of the spectrometer varied considerably with wavelength and was lowest near 0.8 microns for the discrete filter set and at the extremes of the range of the continuous filter. Consequently the spectra are noisier in these regions. The error of the spectra varies from approximately 1 to 5%, dependent on wavelength.

Reference and substrate reflectance

The frost spectra presented are spectral reflectances of the frost samples relative to a freshly smoked MgO surface and, in most cases, are normalized to unity at 1.76 microns. As a MgO surface deteriorates rapidly and is easily contaminated, a rough (powder blasted) gold or silver surface was used as an intermediate standard. These surfaces exhibited nearly uniform angular distribution of reflected light near normal incidence and reflectance, and a small, nearly linear increase in reflectance toward longer wavelengths (16% increase from 0.8 to 2.0 microns).

As both gold and silver mirror surfaces have uniform reflectance throughout the 0.8 to 3.2 micron region, this "redness" of the rough surface is attributed to scattering by surface elements on the order of a wavelength in linear extent.

The reflectance of the stainless steel chambers was near unity. The interior of one chamber was coated with a flat black epoxy paint. The initial reflectance of this surface was 6% (gray) which increased slowly to 21% (gray) during a period of 18 months.

To eliminate any effect of the substrate reflectance sample growth was generally allowed to continue until the frost layers were opaque in the near infrared. The approximate thicknesses required were initially determined by making spectral scans frequently as sample thickness was increased. This was also checked by monitering the reflected intensity near 2.2 microns as the sample grew. The reflectance of a thick deposit is bounded by the reflectances of a thinner deposit of the same material over black and white substrates.

Gas and Liquid Transmission Spectra

Transmission spectra of H_2O vapor and CO_2 gas were made by filling the chamber with a measured pressure of the gas and making a spectral scan of the reference surface. A transmission spectrum of 0.39 m-atm. of CO_2 gas was taken to calibrate the A filter and for band position comparison with the CO_2 frost (Fig. 1). With this equipment, a wavelength shift of the center of the absorption bands could not be detected between the solid and gas phase. A scan of 3 precipitable microns of water vapor showed only faint absorption at 2.7 microns.

To aid in the interpretation of Kuiper's observations, liquid water transmission spectra were also measured (Fig. 1). Spectral scans were made of pools of

water in the bottom of a plain stainless steel chamber. These spectra are not corrected for reflection losses at the water surface. Transmission spectra of 1 and 12 mm of liquid water showed a very sharp decrease in transmission at 1.4 microns and 1.1 microns respectively. The 1 mm and 2 mm water transmission spectra have an additional peak at 1.68 microns which is 60% and 40% respectively of the value of the 0.85 micron peak.

CO_2 frost reflection spectra

Fine CO_2 frosts show a uniform high reflectance from 0.8 to 3.2 microns except near 2.0 and 2.7 microns (Fig. 2a). Increase in the grain size progressively deepens these features and other weaker features appear. Samples with grain size up to 3 mm were grown. The broad absorption feature at 2.9 to 3.2 microns on many of the spectra is due to a small amount of water in the CO_2 source. Frosts grown with a dry ice trap on the CO_2 source gas line (H_2O reduced to about 1 ppm) had 90% reflectance at 3.2 microns (Fig. 2b). The 2.7 micron band is saturated for frosts of grain size larger than about 50 microns and has a minimum reflectance of 1%. The lowest reflectance measured for the 2 micron band was 26% for a fractured 3 mm thick layer (Figs. 2c, 10a). The 1.43 and 1.6 micron bands could be seen only in the very coarsest samples and had maximum absorptions of 6% and 8% respectively. Spectra of commercial dry ice (1 mm grains) are similar to the coarsest frosts grown except for their apparent contamination by water.

Two strong features observed at 2.63 and 2.856 microns and five weak features observed at 1.884, 2.126, 2.295, 2.31, and 3.05 microns do not correspond to CO_2 gas vibrations. The 2.126 and 2.856 micron bands may correspond to slightly shifted $C^{13}O_2$ bands (2.102, 2.83 microns in the gas phase). The

3.05 micron band may correspond to the extremely strong ice ν_3 mode (3.08 μ) but is much narrower than the ice band. The 1.884 and 2.63 micron bands correspond to combinations of the vibration and lattice frequencies (See Appendix IV). Similar combinations have been observed for the ν_2 and ν_3 modes by Osberg and Hornig (1952) and Jacox (1961). Combination with the lattice modes gives an apparent shift to the band position for strong (coarse grained) CO_2 frost spectra but the wavelength of maximum absorption is constant within the resolution of my instrument. No explanation has been found for the features at 2.295 and 2.31 microns.

Fine and medium grained CO_2 frosts showed no appreciable spectral contrast changes at inclinations up to 45° (Fig. 3a, 3b, 3c). At 66°, a small (10%) decrease in spectral contrast was observed (Fig. 3d).

A CO_2 deposit grown at 160° K with no buffer gas was a clear, transparent, specular layer. Due to the large component of specular backscatter not reaching the detector, the deposit decreased the apparent reflectance of the flat black substrate. The clear layer showed the 2.0 micron and 2.7 micron absorption features in about the same proportion as do fine frosts. Growth started at small separated centers on the chamber bottom which expanded until they coalesced. No change in form of the deposit with change in growth rate could be detected, indicating that it grew under near-equilibrium conditions.

H_2O frost reflection spectra

The reflectance spectrum of fine H_2O frosts are dominated by broad absorption features at 1.56, 2.04, and 3.0 microns (Fig. 4). The 2.9-3.2 μ region is saturated for all the frosts observed. All frosts grown in the chamber showed high

reflectance near 1.8 microns and 2.24 microns, but a frost grown outside of the chamber did not. The reflectance maxima at 2.24 microns is typically 90% of the val ue at 1.8 microns. The 2.2 to 2.7 micron region shows the greatest variation between samples. The small increase in reflectance at 2.64 microns is a true maximum only in the finest grained samples (Fig. 5a). For the fine samples, the reflectance increases noticeably toward short wavelengths. This may be the effect of particle size.

The H_2O frosts were generally finer than the CO_2 frosts. It was difficult to grow coarse-grained H_2O frost in the chamber. In order to increase the H_2O concentration, the nitrogen pressure was decreased. However, at initial pressures less than 0.3 torr, the nitrogen gas was rapidly trapped out in the forming H_2O frost, resulting in an uneven frost.

Fine frost which had formed on the outside of the chamber was collected and heaped in the bottom of a clean cold chamber. This sample melted slightly while being transferred. It showed considerably lower reflectance beyond 1.4 microns than did the finer samples. Spectra of fresh melting snow (in situ, Mount Wilson, April 5, 1967) had a reflectance less than 2% throughout the 1.6 to 3.2 micron region.

The change in spectral contrast with inclination is small up to 40° and moderate (15%) at 66° for fine frosts (Fig. 5).

A water deposit grown at 77° K at the minimum pressure attainable had the appearance of glare ice. The chamber pressure during the growth of this sample was less than 0.004 torr. A sharp interference pattern was recorded during the first stages of growth, from which the thickness of the film could be calculated. Visually the sample appeared uniform, transparent and specular. The sample

reflectance was less than that of the black substrate except for a pronounced peak near 3.1 microns (explanation unknown). Continued growth after the addition of one torr of nitrogen resulted in a high reflectance, fine grained frost.

CO_2 - H_2O mixed frost reflection spectra

" A little water goes a long way."

Frosts of several weight fractions of H_2O and various grain sizes were grown. The source gases were let into the mixing manifold simultaneously. At some flow rates and total pressures, some fractionation occurred in the chamber, as evidenced by the formation of two zones of coarse crystals on the chamber wall near a level corresponding to the top of the coolant. The composition in the area viewed by the detector was determined by weighing a sample from this area as it warmed (see Appendix 2). Water had a much stronger effect on the reflection spectra than did CO_2. The strength of the H_2O - CO_2 features depended on grain size. The H_2O features predominated even at low concentrations.

At an H_2O weight fraction of 0.008 (h = .008) all the features of H_2O spectra are present to some extent (Fig. 6). There is about 5% absorption at 1.5 microns, the 2.0 micron band is broadened, the slope from 2.2 to 2.6 microns is increased, and the 3.1 micron region is saturated. There is little left (10% maximum) of the CO_2 reflection beyond 2.7 microns. At h = 0.02, the 1.5 micron absorption has reached 10%. The three minima in the 2.0 micron band characteristic of CO_2 are evident in this fine frost.

As the weight fraction of H_2O is increased, the last distinguishable characteristics of CO_2 which disappear are the detail in the bottom of the 2.0 micron band and the high reflection (greater than 80%) near 2.5 microns. There

is some evidence of the 2.7 micron band in the spectra of all mixed samples.

For coarse grained frosts of h = 0.05 (Figs. 11a, b) the presence of CO_2 is discernible only as small detail at 2.0 and 2.7 microns, but is not apparent at 2.5 microns (Fig. 6c). For $h > 0.05$ (Fig. 7), excepting the 2.7 - 2.8 micron feature, the presence of CO_2 can be established for fine frosts only by the high reflectance near 2.5 microns, and for coarse frosts only by the minor detail at 2.0 microns.

The 2.0 micron detail is due to strong CO_2 absorption and is most marked in the spectra of strongly absorbing, i.e., coarse-grained frosts. In contrast, the high reflectance at 2.5 microns is most evident in the spectra of fine grained frosts. The effect of the increasing strength of the absorption features on the apparent composition is illustrated by the spectra at h = 0.2 and h = 0.23. The coarse grained sample at h = 0.2 (Figs. 7a, 12a, b, c) shows no indication at all of CO_2 except for a small feature at 2.7 microns, whereas the very fine-grained sample of h = 0.23 (Figs. 7d, 11d) shows only weak absorption by H_2O at 1.5 and 2.6 microns.

Sequential samples were grown with H_2O added on top of CO_2 frosts (Fig. 8). For fine frosts, the addition of .0004 g/cm^2 of H_2O on the surface is sufficient to reduce the reflectance 8% at 1.5 microns, broaden the 2.0 micron band, cause an 8% decrease at 2.5 microns and saturate the 3.1 micron region, resulting in a reflection spectrum similar to that for h = 0.008. The addition of 0.007 g/cm^2 yields a spectra almost indistinguishable from pure water.

The addition of 0.18 g/cm^2 CO_2 on top of 0.004 g/cm^2 H_2O resulted in the spectral changes shown in Fig. 9. At the grain size of this sample 0.18 g/cm^2 CO_2 is much more than required for opacity, suggesting that the H_2O features

observed may be the result of water vapor transport from the H_2O frost, high on the chamber walls, to the area observed.

Summary of laboratory spectral measurements

Several conclusions can be drawn from the laboratory results:

1. Spectral contrast is strongly affected by grain size.
2. CO_2 frosts have high reflectance outside the 2.0 and 2.7 micron bands for grain sizes up to at least 3 mm.
3. H_2O frosts have appreciable absorptance near 1.5 and 2.0 microns and beyond 2.3 microns for grain size larger than 10 microns. For grain size larger than 100 microns, reflectance is high only below 1.4 microns.
4. Spectral contrast of fine grained CO_2 and H_2O frosts do not change appreciably at inclinations up to 66° for small phase angles.
5. Small relative concentrations of H_2O have a major effect on the spectra of mixed frosts. This effect increases with grain size. Identification of CO_2 is difficult when H_2O is greater than 10% by mass except at 2.7 to 2.8 microns.
6. Surface additions of small amounts of H_2O will result in H_2O reflection spectra. The alteration is noticeable at 0.0004 g cm^{-2} and complete at less than 0.007 g cm^{-2} for fine frosts.

III. FROST TEXTURE AND SPECTRAL PROPERTIES

Introduction

In previous discussions of the Martian polar caps, details of the physical nature of the deposits have been largely ignored. However, the texture of a frost deposit can affect both its reflection spectra and thermal emissivity and merits more extensive consideration.

An elementary discussion suggests that, if the grain size is larger than the radiation wavelength, the most important textural parameter in determining the reflectance spectrum of a frost is a characteristic "grain size" determined by the volume to surface ratio of the frost. This implies that the textural fine structure will largely determine frost reflectance. The angular dependence of the reflectance of laboratory frosts is compared with the relations for both Lambert reflectance and diffuse isotopic scattering. The laboratory frosts are more nearly Lambert.

In this section it is shown that H_2O frost on Mars will initially be fine-grained, but that little can be said with certainty about the texture of CO_2 frost. The grain size, and hence strength of absorption features, will increase in the Martian spring. Several likely mechanisms for surface concentration of H_2O on CO_2 frosts are discussed. The composition determined by simple interpretation of the resulting spectral reflectance would be misleading. Mean grain size can be estimated directly for laboratory and natural frost deposits; however, the prediction of the mean grain size for Martian frosts requires knowledge of the dependence of grain size on environment. Two useful parameters are developed

to treat this relation, the relative concentration of the condensing gas, and the fraction of the latent heat released at the surface of the frost which is lost by radiation. Changes in rate are treated indirectly by their effects on these two parameters.

There are two major differences between laboratory and natural conditions: control of growth rates and the radiation balance. Under natural conditions, the rate of frost formation is a function of the balance between the atmospheric partial pressure of the condensible gas and the surface crystal temperature necessary to lose the latent heat released. Under the laboratory conditions of this work, the fixed supply rate of gas drives the partial pressure to an equilibrium value. The fixed supply rate can lead to inhomogeneities in the sample, as discussed below. Under natural conditions, terrestrial or Martian, the ultimate loss of latent heat is by radiation or conduction into the gas (crystal formation in clouds), whereas under laboratory conditions all heat is lost by conduction to a substrate. The fraction of heat lost from the growth site by radiation is almost certainly positive and may be near unity for natural frosts, whereas in the laboratory it is negative or, at best, zero.

Three qualitative relations will appear from the following discussions of variations in texture: (1) that the mean grain size will increase with the relative concentration of the condensing gas; (2) that frosts grown by radiative cooling will be finer than those grown by substrate cooling under otherwise equal conditions; (3) that metamorphism will cause grain size increase with time at a highly temperature dependent rate.

Variations in Texture

Dependence of texture on relative concentration

Both laboratory experiments and simple theory indicate that frosts formed from minor constituents are fine grained. It is in general difficult to grow large crystals.

Frost formation requires a net flow of the condensing gas toward the frost surface. If there is a non-condensing gas present, this requires a diffusion gradient which will in turn limit the supply of condensible gas. The partial pressure of the condensing gas will increase linearly (in a one dimensional model) away from the surface of growth. Thus crystals extending above the mean surface will have a more favorable source of gas. This suggests that the crystal size will be proportional to the relative concentration of the condensible gas for a diffusion limited process. Hoarfrosts formed in polar regions exemplify condensation at concentrations of about 10^{-3} to 10^{-4}. They are very fine, open, extremely low density frosts.

In the laboratory an increase in rate results in an increase in temperature at the sample surface and yields a much greater increase in relative concentration. This is the result of the linear dependence of the temperature difference across the sample on rate, and the exponential dependence of the saturation pressure on temperature.

By an analogous process, in the laboratory the relative concentration at the sample surface increases with deposit thickness. This is the result of the greater temperature differential necessary across the deposit to conduct a constant heat load and the consequent increase in saturation pressure.

The effect of radiation cooling versus substrate cooling on texture

Martian frosts will lose heat primarily by radiation, whereas the laboratory frosts lose heat by conduction through the deposit to the substrate. Any resulting difference in surface texture will affect spectral reflectance and must be considered.

For substrate cooling, the heat loss, and hence the growth rate, is controlled by the thermal contact of the growing crystal with the body of the deposit. This limits the distance a crystal can extend above the mean frost surface and favors the growth of the grains which have the best thermal conductivity, i.e., the coarsest grains. Radiative cooling (or conduction by the gas) does not impose these restrictions. Rather, heat is lost most readily by the most exposed surface crystals. This suggests that frosts formed by radiative cooling will be finer grained than those formed by substrate cooling at the same rates and relative concentrations.

CO_2 frost formation on Mars would involve freezing of a nearly pure gas with the latent heat being lost by radiation. This process does not occur naturally on earth and cannot be produced in the laboratory. To do so would require that the gas be contained in a chamber which was no colder than the gas in order to prevent condensation and lowering of the gas pressure. In order that the radiation balance be positive outward, the chamber would have to be situated in an outer blackbody cavity of lower temperature and would have to be transparent in the wavelength regions over which the gas was radiating. For radiation temperatures near 150° K , no practical material fulfills this last requirement. Planets manage to keep the gas from the "cold surface" at infinity by gravitation. There is no obvious way by which this process can occur on less than a planetary scale.

In theory, frosts forming from a pure gas by radiation cooling could have

an upper permeable, isothermal region and a lower impermeable region with thermal gradients, or only one of these. However, the high visual albedo of the Martian caps imply that they have a highly scattering, and therefore probably permeable, surface layer.

Metamorphism and sublimation

Metamorphism of terrestrial snow is dominated by two processes, the growth of large grains at the expense of smaller ones, and the transformation of elaborate grains of large surface area (powder snow) to compact, equidimensional grains of low surface area. Both processes are the result of the lower free energy of surfaces of larger radius of curvature, or on a molecular scale, the greater stability of a molecule located in an extended surface relative to one located at a lattice edge or corner.

The rate of metamorphism increases with vapor pressure and reaches a maximum when net sublimation (or melting) occurs. This is demonstrated terrestrially by the much more rapid metamorphism of temperate relative to polar snows. Thus metamorphism can be equated to an increase of mean grain size (volume to surface ratio) and is strongly temperature dependent.

This suggests that any increase in grain size of Martian CO_2 polar frosts would occur at a relatively steady rate because the temperature is fixed, whereas for Martian H_2O frosts the change in grain size would increase greatly just prior to sublimation or melting when the temperature increases.

The effect of gas (wind) velocity at the frost surface on grain size is not readily assessable. Under terrestrial conditions, the major effects of wind are to impose a strong orientation on growing frost deposits, to break up fragile crystal forms, to drift new falling snow, and to glaze and pack existing snow surfaces.

None of these appear to alter the mean grain size in a significant or predictable manner.

Variations in spectral properties

Dependence of spectral reflectance on grain size

The strength of the absorption features observed in the laboratory increases with grain size. This results from the increasing path length through the grains before light is scattered out of the frost. The intensity of the reflected light is controlled largely by the nature of the surface (first optical depth) of a frost layer.

For particulate scattering, the major parameter is the albedo for single scattering, ϖ. This is the ratio of the probability of scattering to the probability of scattering or absorption. As the mean path length through the particles (grain size) increases, ϖ decreases asymptotically from unity to the reflection coefficient of the material and the reflectance of the deposit decreases rapidly. In the theory of particulate scattering, the distance between scattering events has no effect. This suggests that the spectral reflectance of frosts and clouds will be the same if they have identical composition and grain size. Though it has been assumed that the emissivity of Martian CO_2 frosts would be near unity (see for example Leighton and Murray, 1966) this might not be the case. The emissivity of Martian frosts and the radiation balance over the polar cap are discussed in Appendix III.

Angular dependence

As it is difficult to measure spectral reflectance in the laboratory with the

same illumination and observation angles as occur in observation of Mars, extrapolation of the laboratory results to low angles is desirable. Two theories are considered for this extrapolation, Lambert reflectance and diffuse isotropic reflectance (Chandrasekhar, 1960). To test how well the laboratory frosts agree with these theories, the spectral backscatter from two samples, fine H_2O and fine CO_2 frost, was measured at several inclinations. The gray variations in intensity could be eliminated by considering spectral contrast, that is, the spectral reflectance normalized to its maximum value. It is spectral contrast that is appropriate to the Martian observations. Spectral contrast does not change with inclination for Lambert reflectance, whereas it decreases with inclination for isotropic diffuse reflectance.

The laboratory measurements are compared with the theoretical relations in Fig. 13. It should be observed first that the variations of spectral contrast are small relative to the magnitude of the features in both the laboratory and the Martian cap spectra. The laboratory frosts are more nearly Lambert than diffuse. The behavior on the edge of the extremely strong 3-micron band of H_2O is anomalous. If the Martian frosts show the same small decrease in spectral contrast as do the laboratory samples, the laboratory measurements of normal backscatter and the Martian observations can be directly compared.

Summary: The composition, texture, and reflectance of Martian frosts

The two probable compositions of the polar caps are predominately CO_2 and entirely H_2O. These two cases are discussed individually below in detail. The possibility that much or most of the condensation takes place in the form of clouds

is common to both. It will be difficult, if not impossible, to distinguish clouds from fine frosts spectrally. The variation of texture with season must be considered, particularly for H_2O frosts, which have sufficiently large absorption coefficients at nearly all wavelengths under consideration to result in a strong dependence of reflectance on grain size.

It is certain that H_2O frosts on Mars would be fine grained when they form. Though the unique circumstances of CO_2 frost formation on Mars prevent simple theoretical calculation of texture; the high visual albedo of the Martian caps implies they are not thick, non-scattering layers and that the laboratory measurements would apply to Martian CO_2 frosts.

CO_2 polar caps

The first frost formation in the fall would be pure H_2O. Once the temperature of CO_2 condensation is reached, the H_2O/CO_2 ratio for frost formation could be no more than 10^{-6}. The concentration in the cap during the fall and winter season could be increased only by snowfall enriched in H_2O. If this occurs, its maximum rate should occur over that part of the polar region where the initial cooling of temperate air occurs. It is likely that the H_2O concentration will generally increase toward lower latitudes. It is quite possible that an annular "polar cap" of pure H_2O would form. However, of the total material condensed during a winter, the fraction which is H_2O will certainly equal or exceed the H_2O - CO_2 mixing ratio in the temperate regions, observed to be about 10^{-4}.

During the CO_2 sublimation cycle, the H_2O/CO_2 sublimation rate is

again 10^{-6} if the air is not stirred. However, an influx of temperature air saturated with H_2O into the polar region could cause net H_2O deposition. This H_2O would be concentrated at the cap surface. H_2O deposition could continue until after all the CO_2 had sublimed.

Another process which could enhance the H_2O features in the reflection spectrum is sublimation-condension (vapor transport) on a daily time scale. The heat balance of exposed areas will go through a greater daily range than that of shadowed areas, allowing the same process of H_2O enrichment which occurs on a seasonal time scale to occur on a daily time scale preferentially on exposed areas which slope sunward. These are of course also the areas which are viewed preferentially from the earth. This process would have its maximum effect on the observed spectrum at high latitudes and in the late spring, just the conditions under which the spectra of the cap have been obtained. This suggests that if the polar cap reflection spectra ever show H_2O features, they will be most pronounced in the polar spring. The expected increase of grain size during the spring cycle would enhance the spectral contrast of these features.

H_2O polar caps

Water frost formation on Mars is analogous to frost formation under terrestrial polar conditions. The condensing gas is a minor component (10^{-4} on Mars at 190°K, 10^{-4} on earth at -40°C) and the frost grain size is expected to be very fine. Formation of the caps by snowfall would also yield fine crystals. The temperature of the forming cap could range between 145°K (CO_2 freezes) and 198°K (saturation temperature for 10 percipitable microns of water vapor in the atmospheric column). It is difficult to imagine some process by which the vapor pressure

over the forming cap could be greater than in the temperature regions. The cap temperature would probably be somewhat less than 190°K due to the formation of diffusion gradients and the consequent lowering of the H_2O vapor pressure near the surface.

Schorn et al. (1967) estimate the amount of H_2O in the polar caps as .025 g cm^{-2} (15 precipitable microns over the entire planet condensing into a cap of 30° radius). As a fine frost this amount is ample to give a high reflectance in the visual and be optically thick in the near infrared even when lying over a dark substrate. The temperature of the H_2O frost could vary daily, in contrast to CO_2 frost. The increased solar flux onto areas inclined sunward would probably result in appreciable H_2O transport from equitorial facing slopes and surfaces to the more shaded polar facing areas. As the frost in the shaded areas would be largely hidden from terrestrial observers, this process need occur over only short distances (the scale of the roughness) to result in an apparently rapid spring recession of the polar cap. During the spring ablation cycle, the frost temperature could rise until the water vapor pressure equaled the total pressure (at 6°C). However, any stirring of the air or any diffusion gradients would lower the water partial pressure and hence the temperature (.025 g = 21 meters at 10 mb). In analogy with terrestrial polar snow, the grain size would probably increase during the subliming cycle.

IV. CONCLUSIONS

Introduction

The comparison of the experimental results to Martian spectra depends strongly on the assumption that the reflection spectrum of a frost is determined by the physical nature of the frost without regard to how the frost arrived at that state, and that this can adequately be described by the two parameters, composition and grain size.

Certain properties of the Martian polar regions cannot be duplicated in the laboratory (Section III) and others are unknown. It is almost certain that some of these are important to the frost growth processes on Mars and the possibility that their effects are other than one would predict must be remembered. The variations in form of terrestrial snow crystals and snow deposits are great and many are not yet understood (see, for instance, Mason, 1957). There is no a priori reason to expect that the grain size, if not the composition, of the surface of the Martian polar caps does not change seasonally or even more rapidly.

The measured spectral contrast for backscatter from fine frosts did not vary significantly for inclinations less than 65°. This is 10° greater than the inclination of the edge of the Martian cap at the time of its largest apparent size during the 1969 opposition. It thus appears likely that the spectral contrasts of frosts grown in the laboratory are directly applicable to the observational geometry of Mars. However, there is no obvious method of demonstrating that Martian frosts do not have significantly different low angle backscatter. (One crystal form observed for cubic lattices is a skeletal cube. Corners of this form have an extremely anisotropic scattering phase function.)

Interpretation of existing Martian polar cap spectra

Moroz reported that the spectrum of the polar cap was less intense in the 1.5-1.8 micron interval than the spectrum of the central region of Mars and that the 1.4 micron absorption band was displaced toward longer wavelengths (1.5 microns). Unfortunately he did not obtain sufficient data to allow reduction of his cap spectrum to spectral reflectance. However, an estimate of the spectral reflectance of the polar cap can be obtained from Moroz's data by normalizing the cap spectrum against the spectrum of the center of the planet. This assumes that the center of the disk is grey in this wavelength region and that the atmospheric transparency was the same on the nights of both observations. These are both poor assumptions. The resulting spectrum is compared with representative laboratory results in Figure 14. The peak at 1.3 microns is almost certainly spurious. The remainder of the cap spectrum is in reasonable agreement with the coarsest H_2O frost measured (which was grown from the atmosphere and allowed to melt slightly) and indicates the presence of medium-grained (0.05 to 0.1 mm) H_2O frost. The observations by Kuiper imply a similar result.

However, the amounts of H_2O as a surface concentration required to yield such spectra are less than 0.005 g cm^{-2}. For comparison, the amount which would be trapped in the simplest CO_2 cap model is about 0.01 g cm^{-2}. Thus, the reported observations of H_2O absorption features in the spring do not establish that the polar caps are composed primarily of H_2O. Such features are compatible with a predominately CO_2 cap model after a modest amount of CO_2 sublimation has occurred.

Future observations

Neither Moroz nor Kuiper made measurements at the optimum time for polar cap observation and the apparent size of the polar cap was far from its maximum (e.g., only one-quarter of the maximum size to be attained in 1969). Future observations are clearly desirable. They should be made at times and in wavelength regions which will be most diagnostic of the composition of the polar cap.

The spectral measurements indicate that it will be easiest to detect the presence of solid CO_2 as a fine frost. Martian frosts should be at their finest during the accumulation phase of the polar cap. H_2O can be most definitely identified as a strongly absorbing frost. This would occur during the sublimation phase. As the detection of CO_2 frost would determine the composition of the Martian caps to first order whereas detection of H_2O would not, the most helpful observation would be of the accumulation phase.

In light of the preceding discussions of textural effects and the uncertainty of predicting the grain size of Martian frosts, it seems best to design an observation whose success is as independent of grain size as possible. In particular, one should allow for H_2O frost being fine-grained and CO_2 frost coarse-grained. This makes interpretation of the spectrum the most difficult. Wavelengths shorter than 1.3 microns are of little use as both H_2O and CO_2 frost have high reflectance and show no reliable absorption features.

Earth based observations of Mars can be made only at those wavelengths where the atmospheres of both planets are transparent. The spectra of CO_2 and H_2O frost are compared with the Earth atmospheric window in Figure 15 (I have used 75%

transmittance as the window limit). At the low pressure and temperature of the Martian atmosphere, the CO_2 absorption bands (Figure 16) are much narrower than under terrestrial conditions (e.g., compare with Figure 4, Appendix 3), and the only further reduction of the windows they cause is to move the terrestrial limit at 2.08μ to about 2.1 μ. The spectrum adopted for the Martian atmosphere is based on the data of Stull et al. (1963), for 100 m-atm of CO_2 at 0.01 atmospheres pressure and 250°K temperature. The CO_2 path length appropriate for polar cap observations is about 500 m-atm (80 m-atm column, 2 pass, sec z=3), five times the maximum amount for which tables are available.

There are two regions of interest, 1.48 to 1.76 microns and 2.1 to 2.47 microns. Distinction between coarse-grained CO_2 and fine-grained H_2O frost would be most certain from 2.2 to 2.47 microns, where CO_2 frost has no absorptance and the reflectance of very fine H_2O frost decreases from 99% to 83% toward longer wavelengths. A resolution of about 0.08 microns would be desirable. Distinction between coarse CO_2 and fine H_2O frost would be difficult in the 1.5 micron band or 2.1 to 2.2 micron interval, even with better resolution. Measurements without some spectral resolution across the windows would be of limited use as they may be very dependant on the scattering phase function.

From outside the earth's atmosphere the picture is much brighter (Figure 16). The presence of H_2O could be detected by photometry or spectrometry at 1.6 or 2.5 microns. The 3.0 to 3.2 micron region would allow an extremely sensitive test for H_2O. Only from outside the earth's atmosphere would positive identification of CO_2 frost absorption features be possible by observing the 2.63 micron lattice vibration combination feature.

Thermal flux as a diagnostic test

One distinction between the H_2O and CO_2 cap models is the infrared flux at the frost surface. The brightness temperature for a CO_2 cap ($\epsilon < 1$) will be less than 145°K at all times. The brightness temperature for an H_2O cap ($\epsilon \simeq 1$) would be about 170° to 190°K during the accumulation season and could be up to 0° C during the sublimation season. Thus a determination of a polar cap brightness temperature of more than 145° K is a critical test of the absence of CO_2.

Such a measurement should be made outside the absorption bands to avoid the effect of the atmosphere, and at a time without clouds in the observation path. Measurement of either 7 micron or 22 micron flux would be a sensitive test, as H_2O frost radiates well at both wavelengths and CO_2 frost does not.

From outside the earth's atmosphere, the most diagnostic test, but one requiring sensitive instrumentation, would be the flux density at 6 to 7 microns. This is the center of the υ_2 band of H_2O ice and is halfway between two CO_2 bands. The emissivity of H_2O frost would almost certainly be near 1. Since the substrate will be at nearly the same temperature, a thin deposit will not affect the result if the substrate emissivity is also high (appropriate for rocks). The emissivity of CO_2 frost would be low, and the deposit would almost certainly be thick for most of the winter. The black body flux in this interval is 10^{-6} watt cm^{-2} at 145° K and 35 times greater at 190°K. It is extremely unlikely that the flux ratio will be less than 35 for H_2O frost at 190° K vs CO_2 frost at 145°K. The corresponding ratio for H_2O at 170° ($p_p = 6 \times 10^{-6}$ torr) is 7.5.

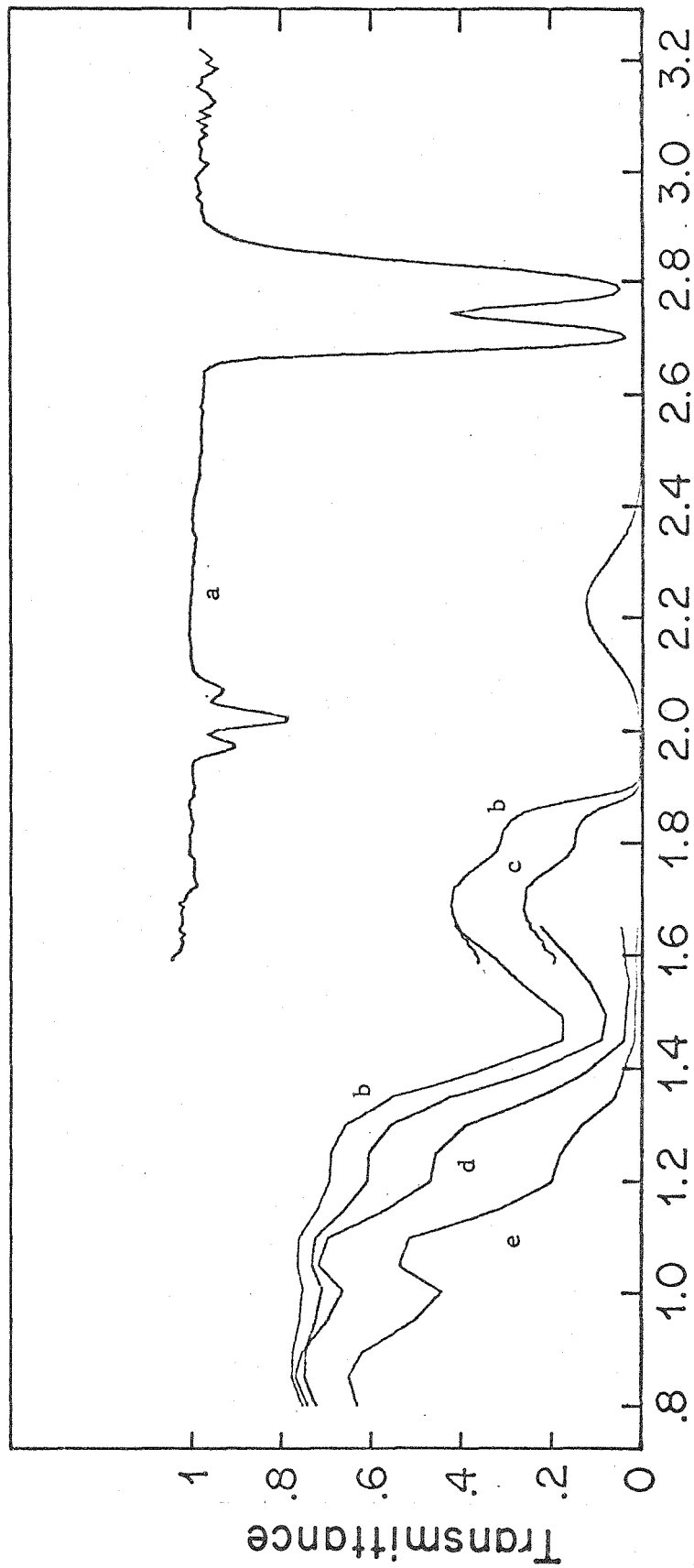

Figure 1. Transmission spectra of CO_2 gas and H_2O liquid. (a) 0.39 m-atm. of CO_2 gas. (b) 0.1 cm water. (c) 0.2 cm water. (d) 0.4 cm water. (e) 1.2 cm water.

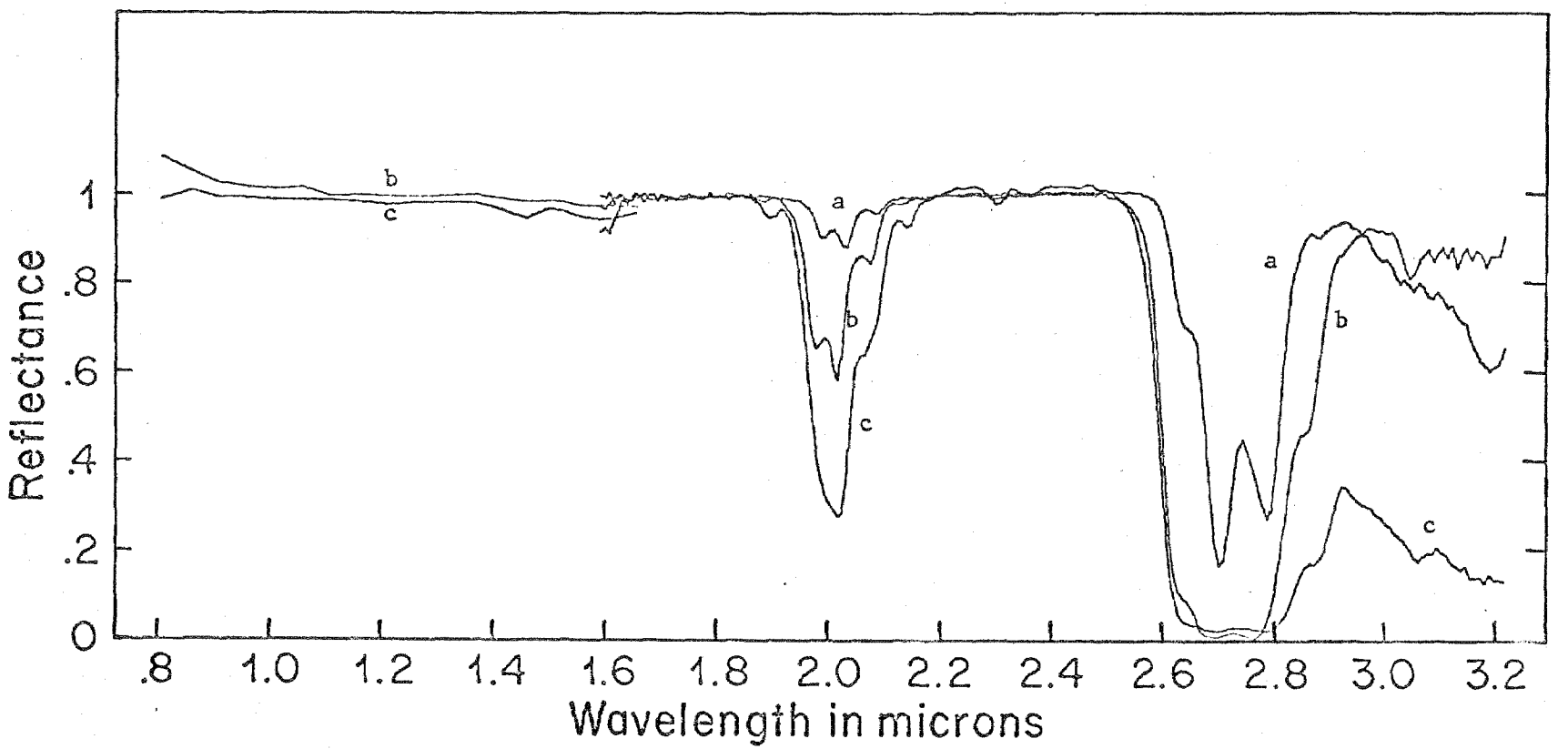

Figure 2. Spectral contrast of CO_2 frosts. (a) Fine-grained frost. (b) Medium-grained frost, H_2O about 1 ppm. (c) Fractured layer, 3 mm thick. (Figure 10a).

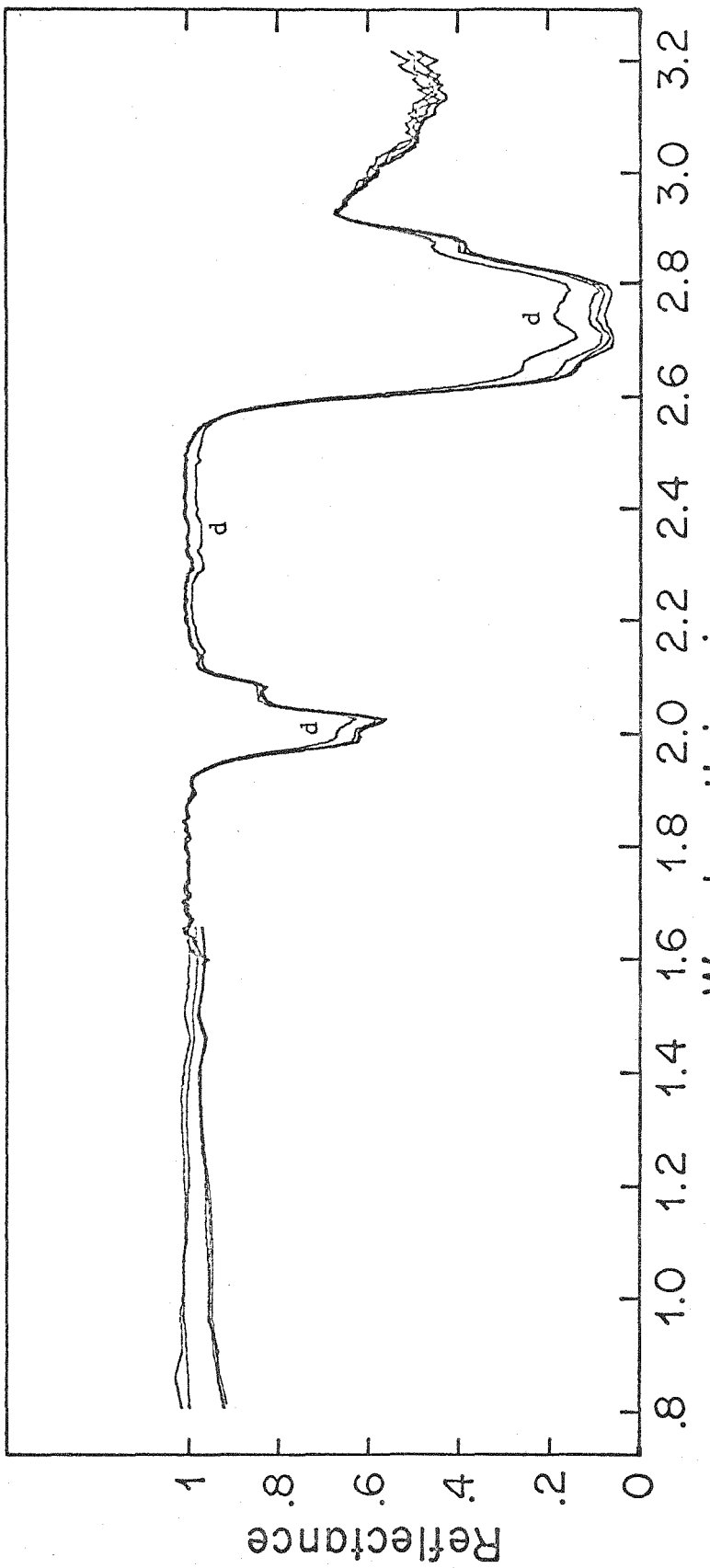

Figure 3. Spectral contrast of a medium-grained CO_2 frost (1 mm thick) at 0^o to 66^o inclination. (a) $i = 0^o$. (b) $i = 20^o$. (c) $i = 45^o$. (d) $i = 66^o$.

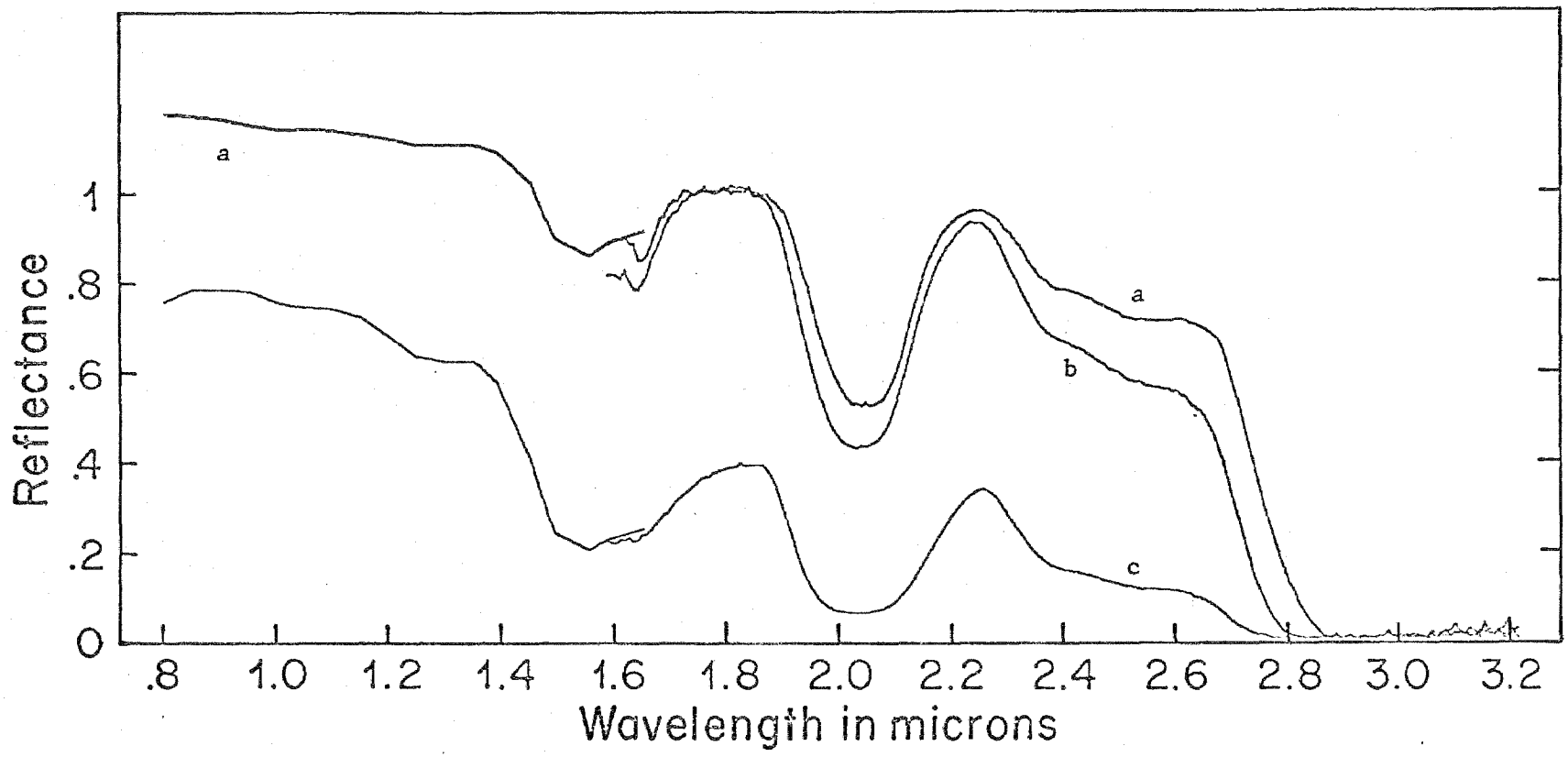

Figure 4. Spectral contrast of H_2O frosts. (a) Very fine-grained frost, 0.004 g/cm^2. (Figure 10c). (b) Fine-grained frost (Figure 10d). (c) Medium-grained frost, collected from outside of the chamber . Scale of curves (b) and (c) are the same.

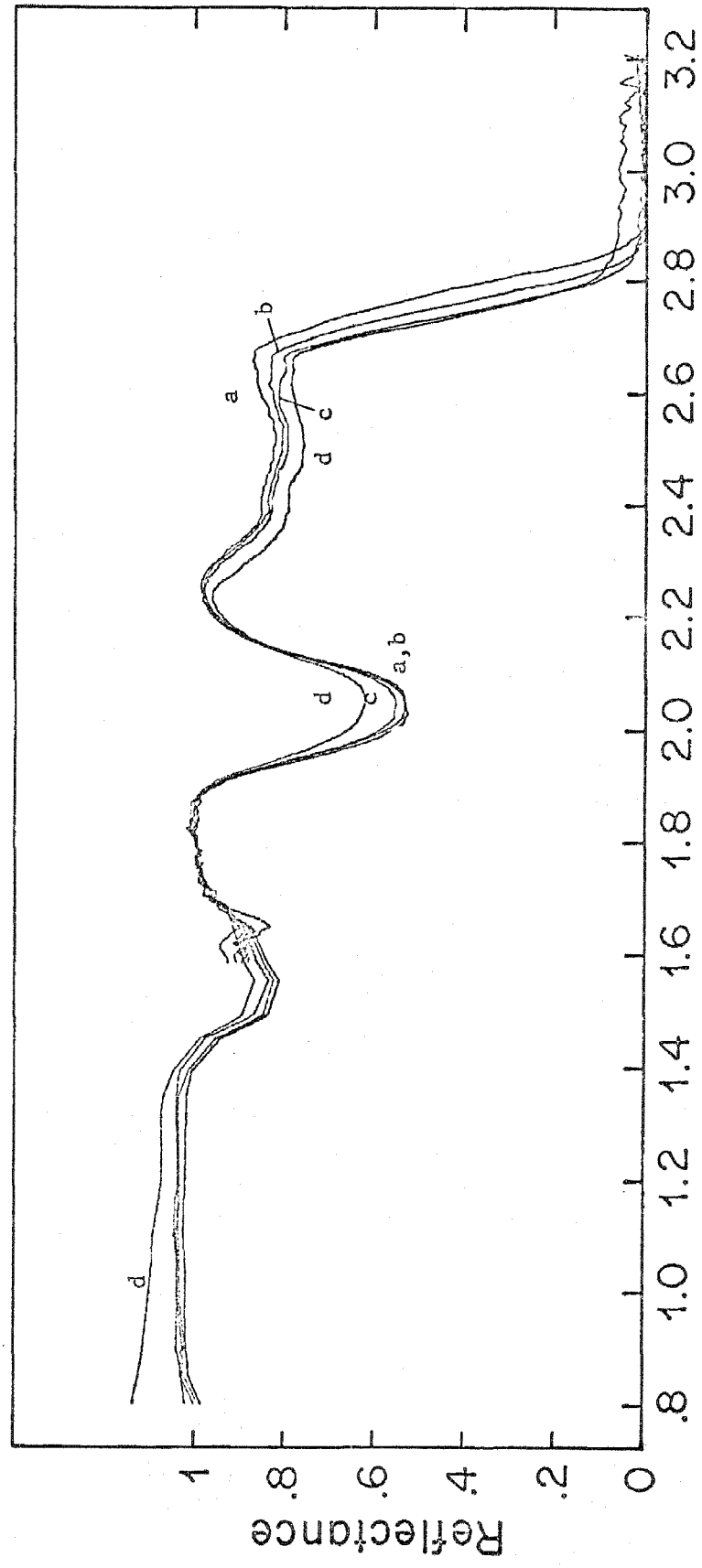

Figure 5. Spectral contrast of a fine-grained, 1 mm thick, H_2O frost at 0° to 66° inclination. (a) $i = 0^\circ$. (b) $i = 20^\circ$. (c) $i = 40^\circ$. (d) $i = 66^\circ$. (The rise below 1.4 microns is probably due to bad data.)

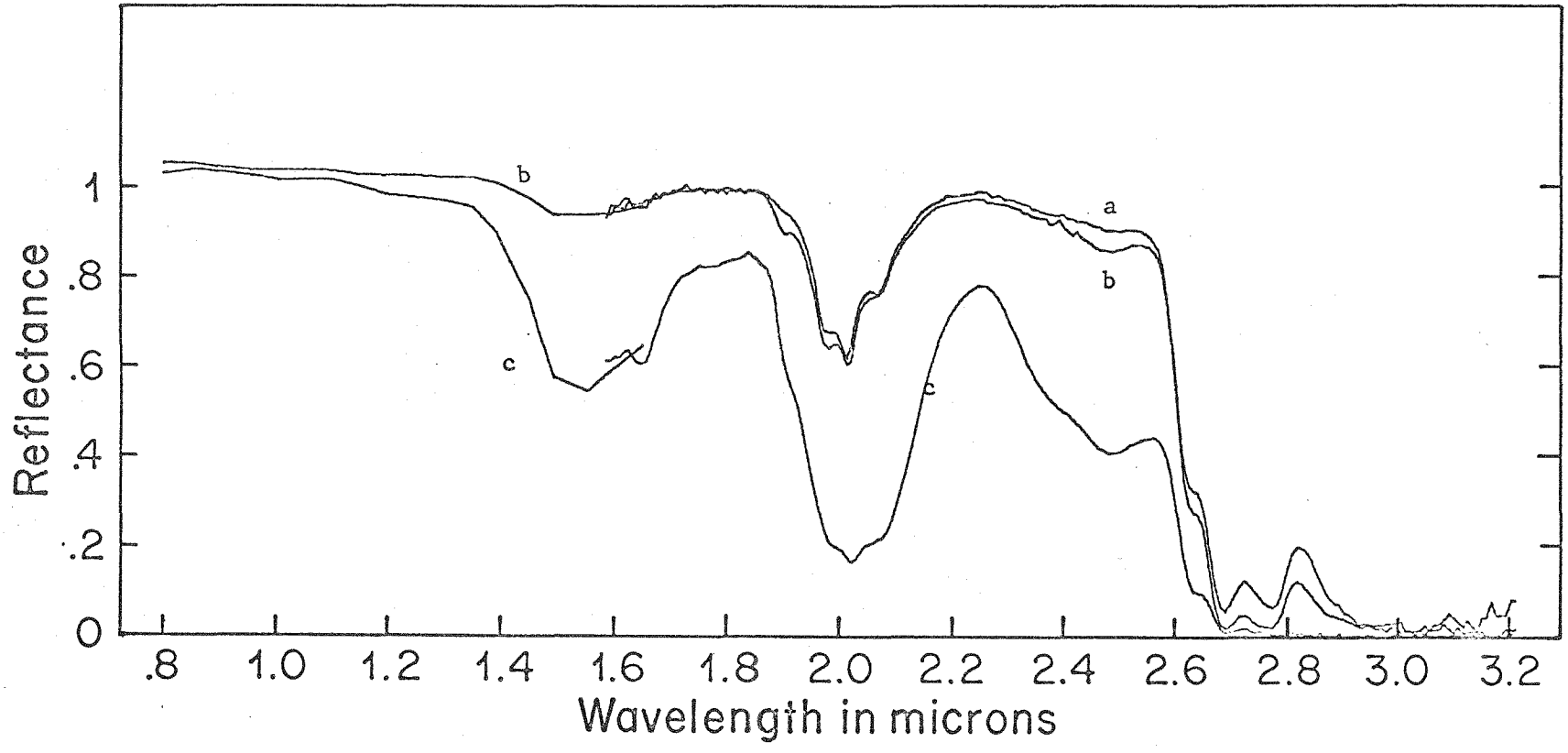

Figure 6. Spectral contrast of mixed frosts of H_2O weight fraction 0.008 to 0.05. (a) h = 0.008, fine-grained frost. (b) h = 0.02, fine-grained frost. (c) h = 0.05, coarse-grained frost. Curve (c) is normalized to curve (b) at its maximum. (Figure 11a,b).

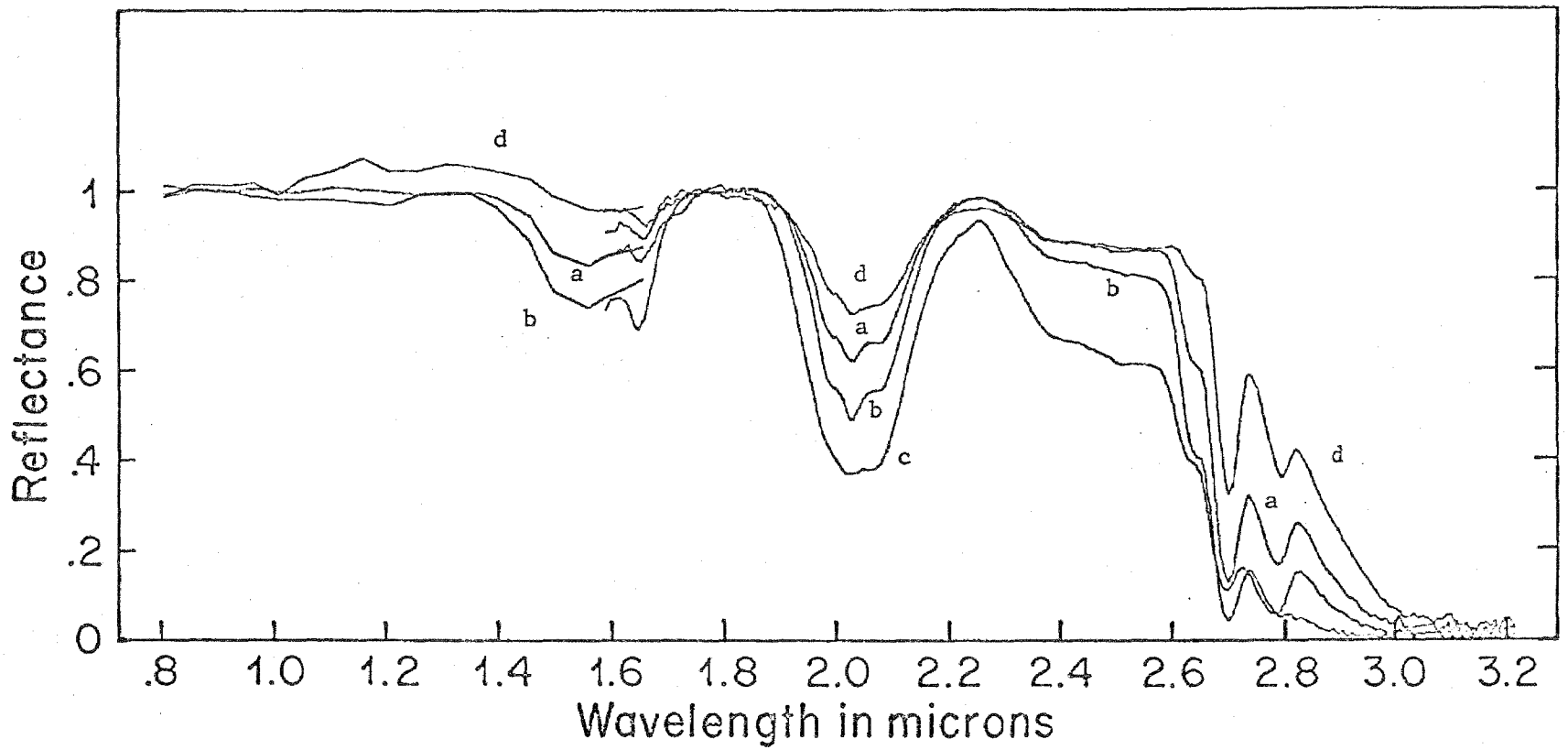

Figure 7. Spectral contrast of mixed frost of H_2O weight fraction 0.1 to 0.23. (a) h = 0.1, fine-grained frost (Figure 11c). (b) h = 0.1, medium-grained frost. (c) h = 0.2, coarse-grained frost (Figure 12 a,b,c). (d) h = 0.23, very fine-grained frost (Figure 11d).

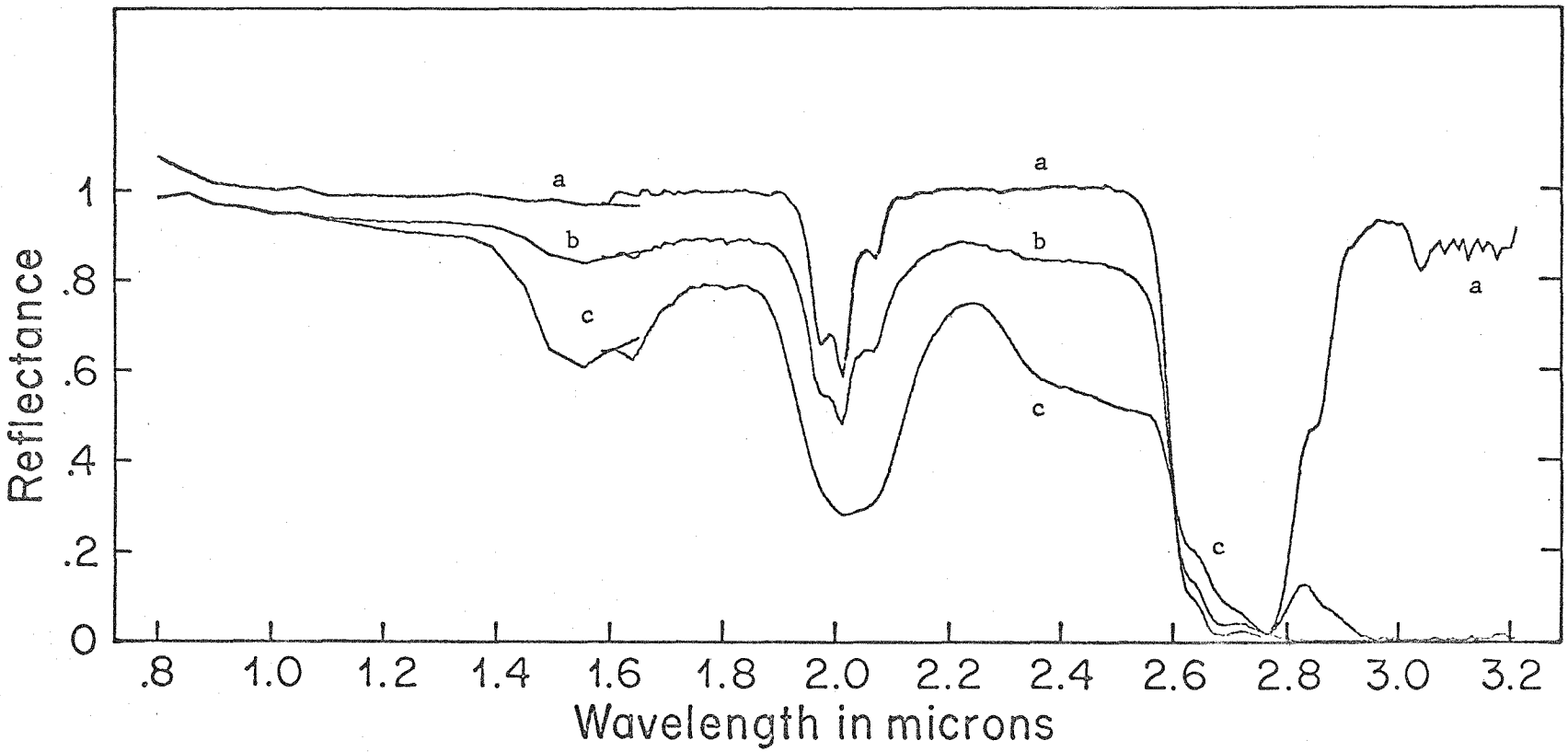

Figure 8. Spectral reflectance of CO_2 frost with surface addition of H_2O frost. (a) CO_2 frost, H_2O about 1 ppm. (b) CO_2 covered by 0.0004 g/cm^2 H_2O frost. (c) CO_2 covered by 0.007 g/cm^2 H20 frost. Curves (b) and (c) are normalized to 1 maximum.

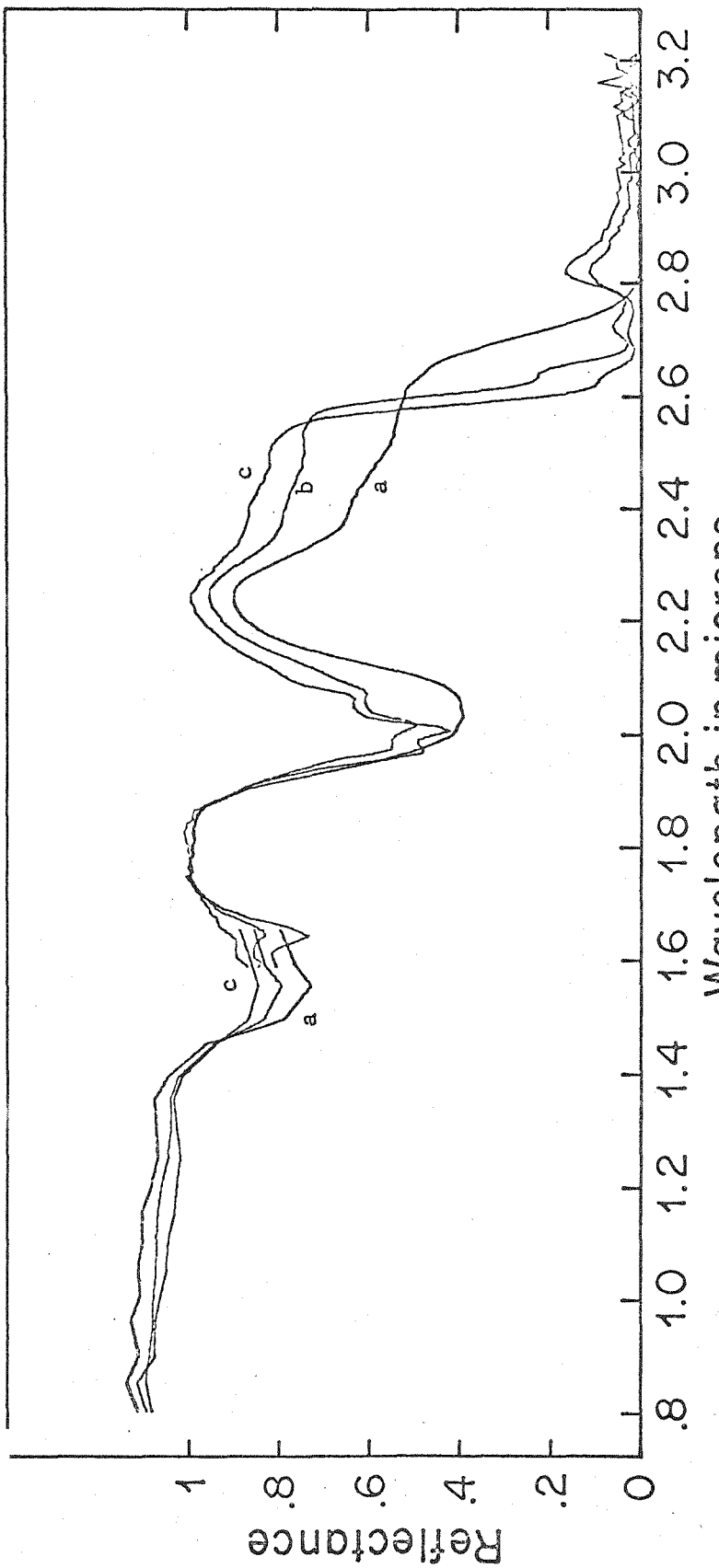

Figure 9. Spectral contrast of H_2O frost with surface addition of CO_2 frost. The CO_2 may be contaminated by H_2O. (a) H_2O frost, 0.004 g/cm^2. (b) H_2O covered by 0.05 g/cm^2 CO_2 frost. (c) H_2O covered by 0.18 g/cm^2 CO_2 frost.

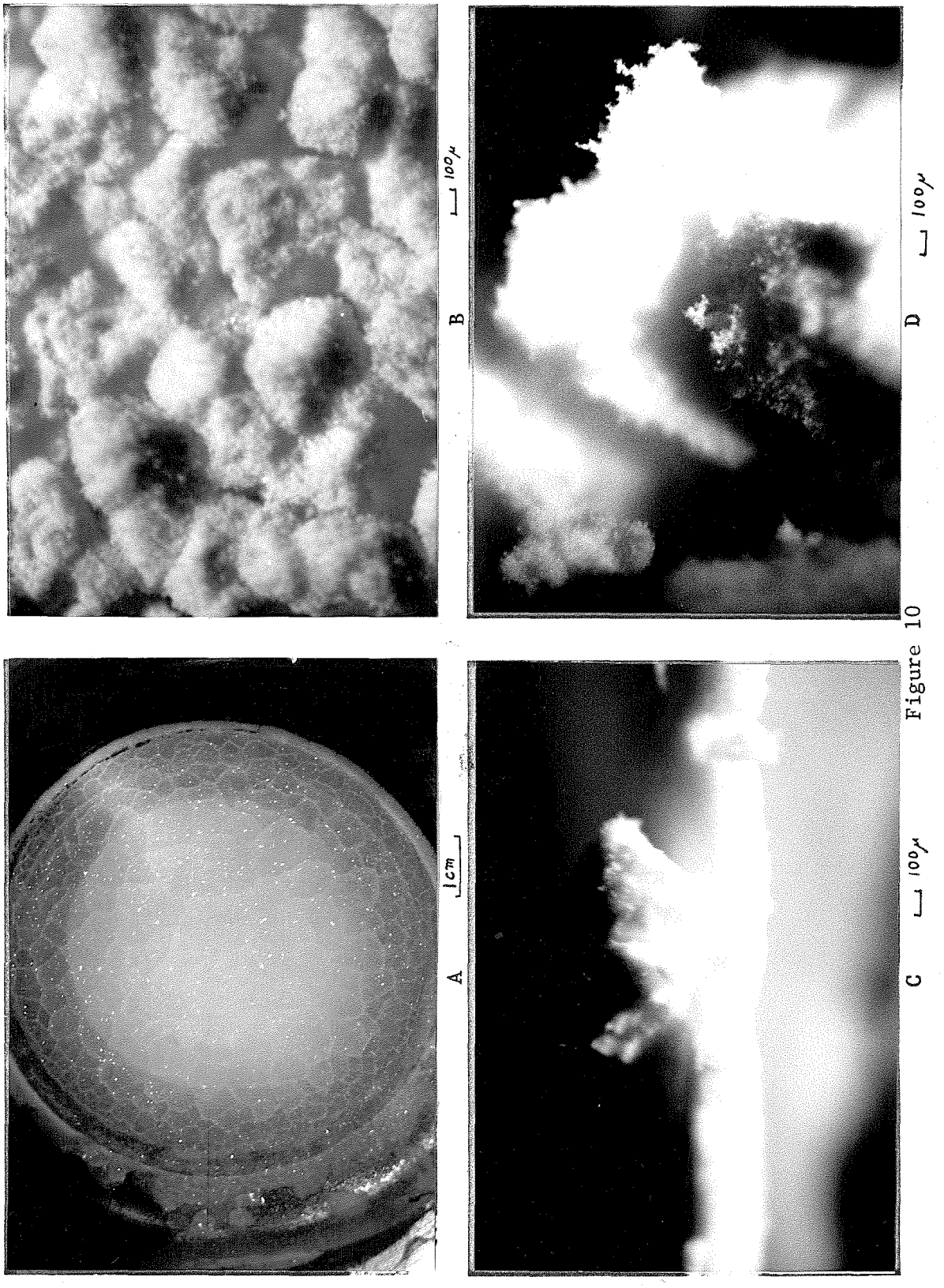

Figure 10

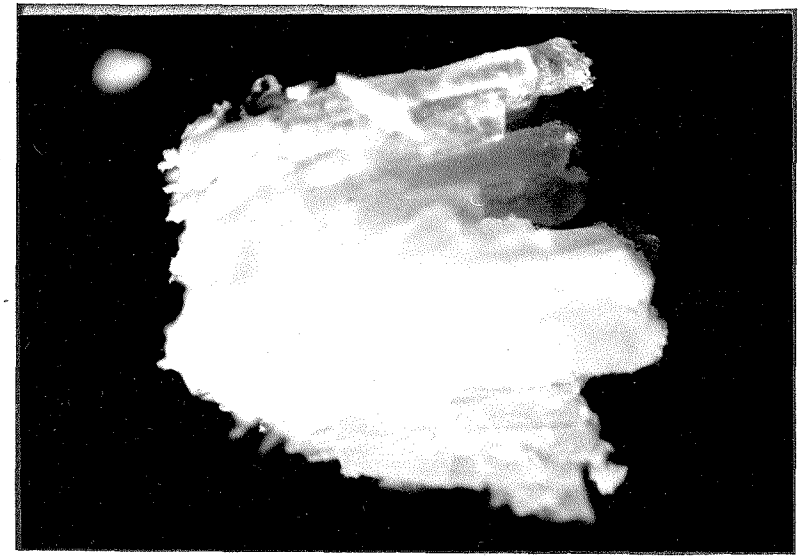

A

B

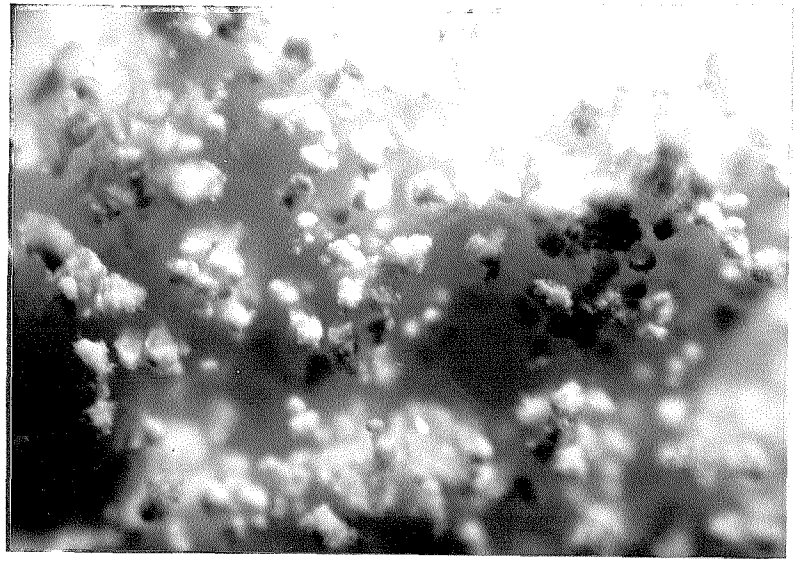

C

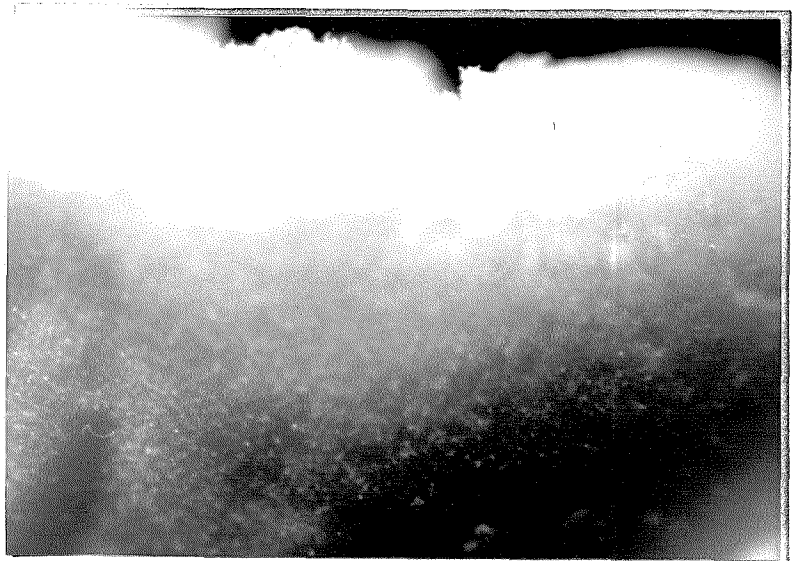

D

Figure 11 ـــ 100μ

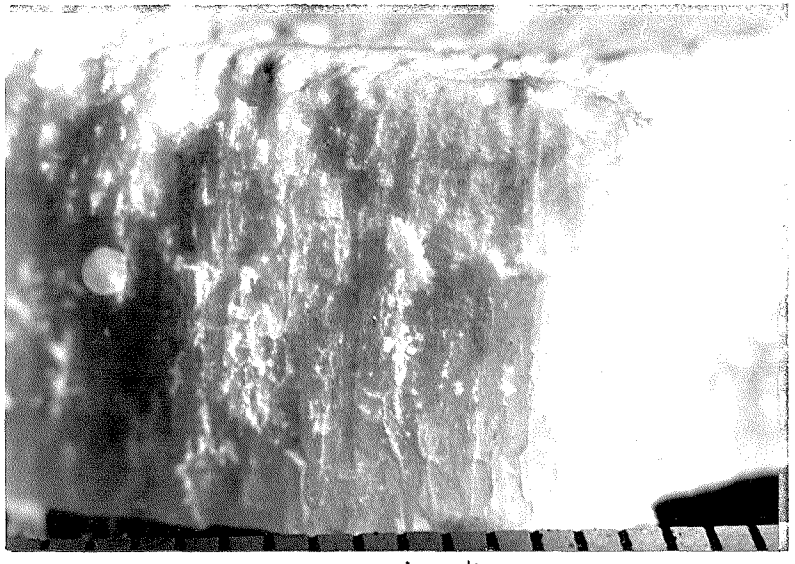

A 1mm

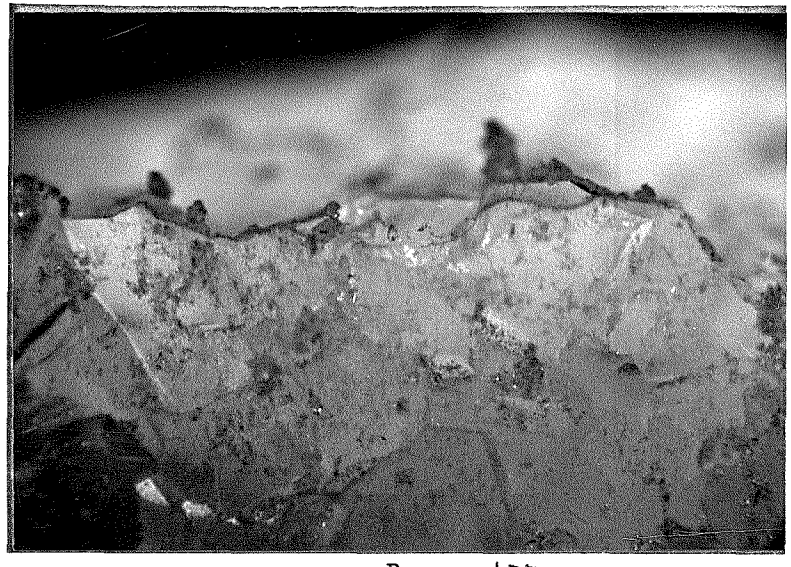

B 1mm

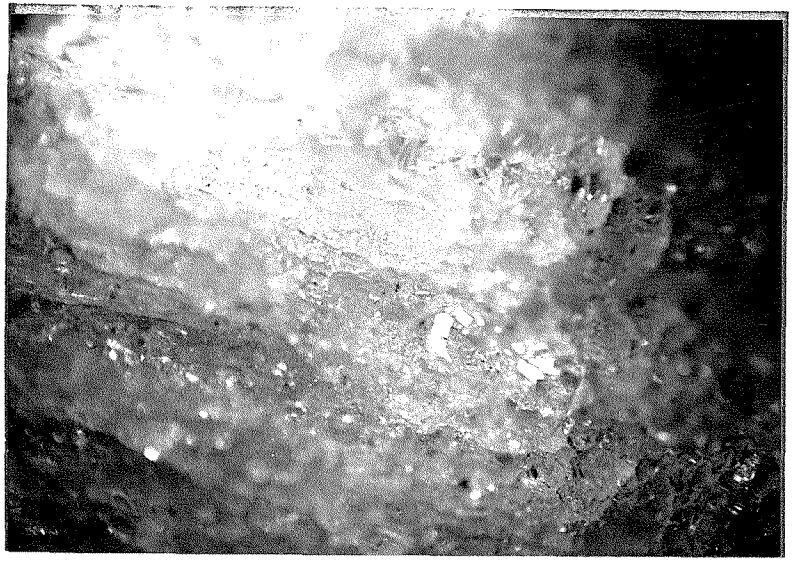

C 1mm

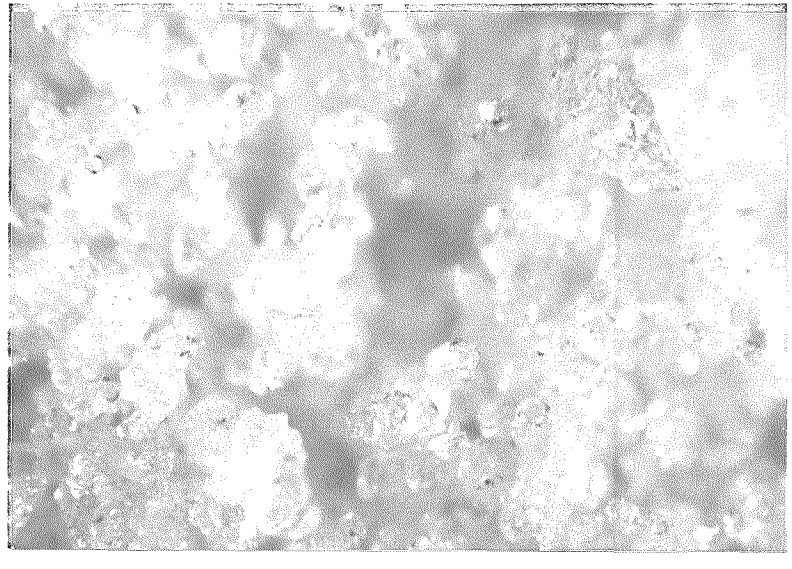

D 100μ

Figure 12

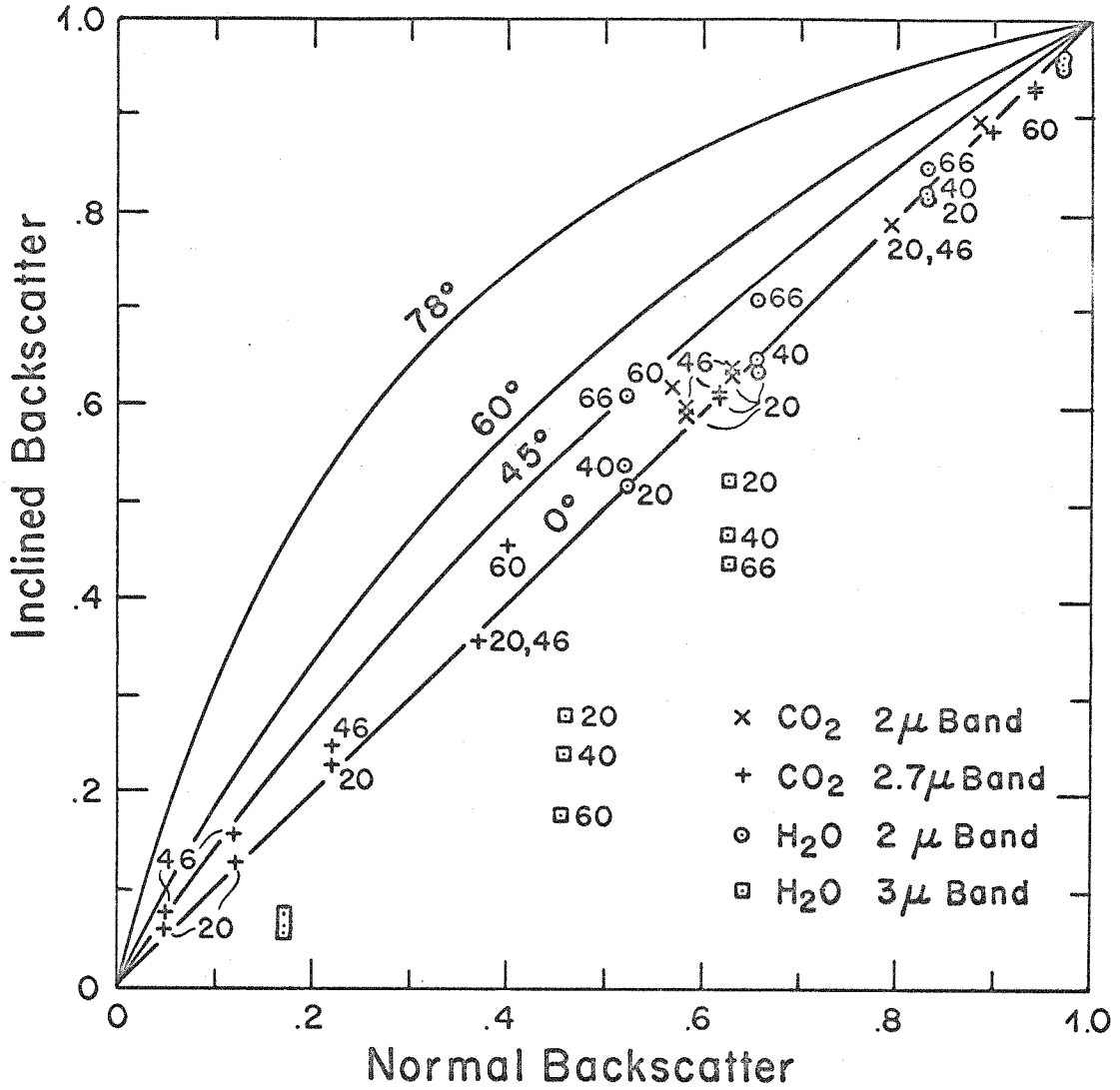

Figure 13. The dependence of backscatter spectral contrast on inclination. The theoretical relation for a thick isotropic layer at 45, 60, and 78 degrees inclination and laboratory determinations for fine H_2O and CO_2 are shown. The laboratory values for 60 and 66 degrees may be slightly high due to scattering from the exposed chamber bottom. The spectral contrast is the same at all inclinations for Lambert scattering.

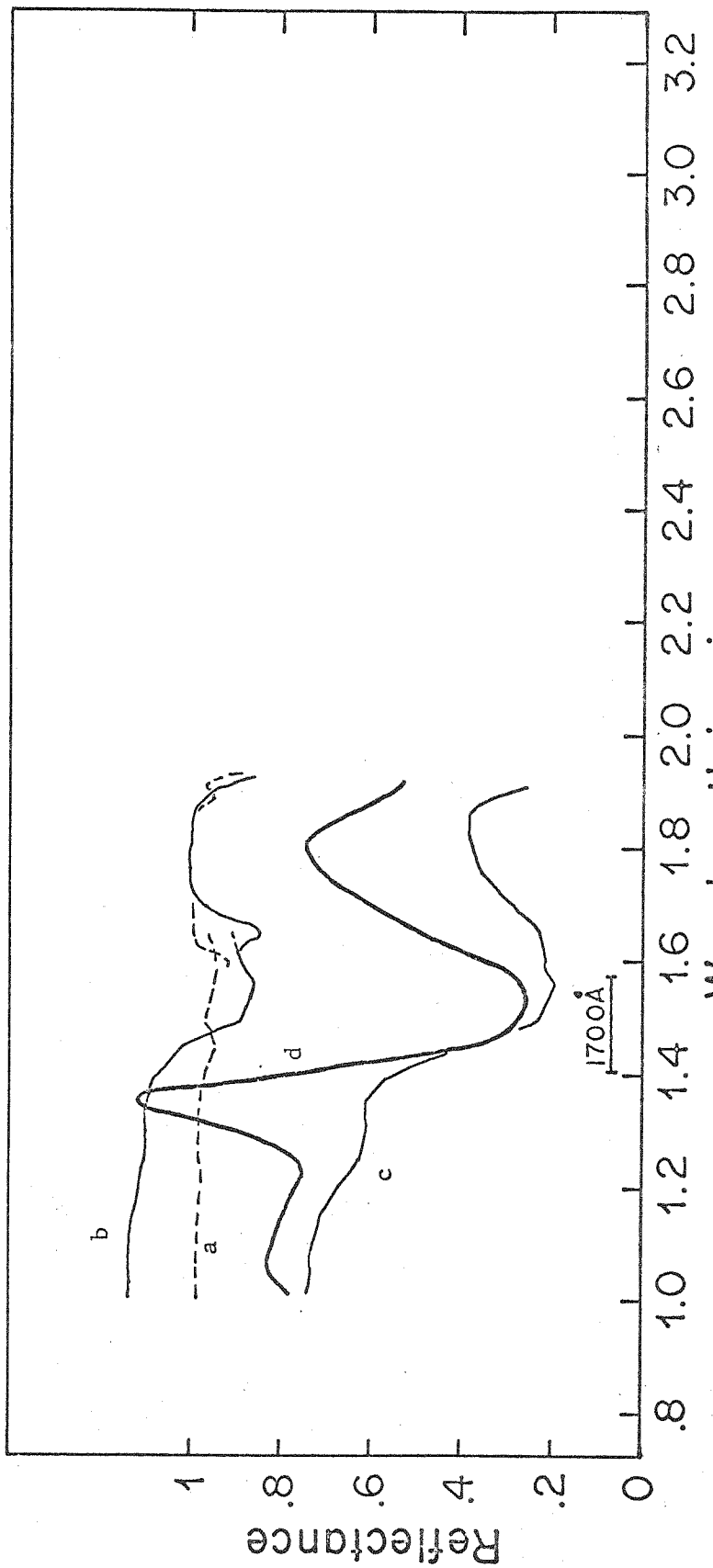

Figure 14. The cap/disk spectrum of Mars compared to representative laboratory frost spectra. (a) Very coarse-grained CO_2. (b) Very fine H_2O frost. (c) Medium-grained H_2O frost. (d) Ratio of the polar cap to the central area of Mars based on spectra obtained by Moroz. The bar indicates the resolution of Moroz' spectra.

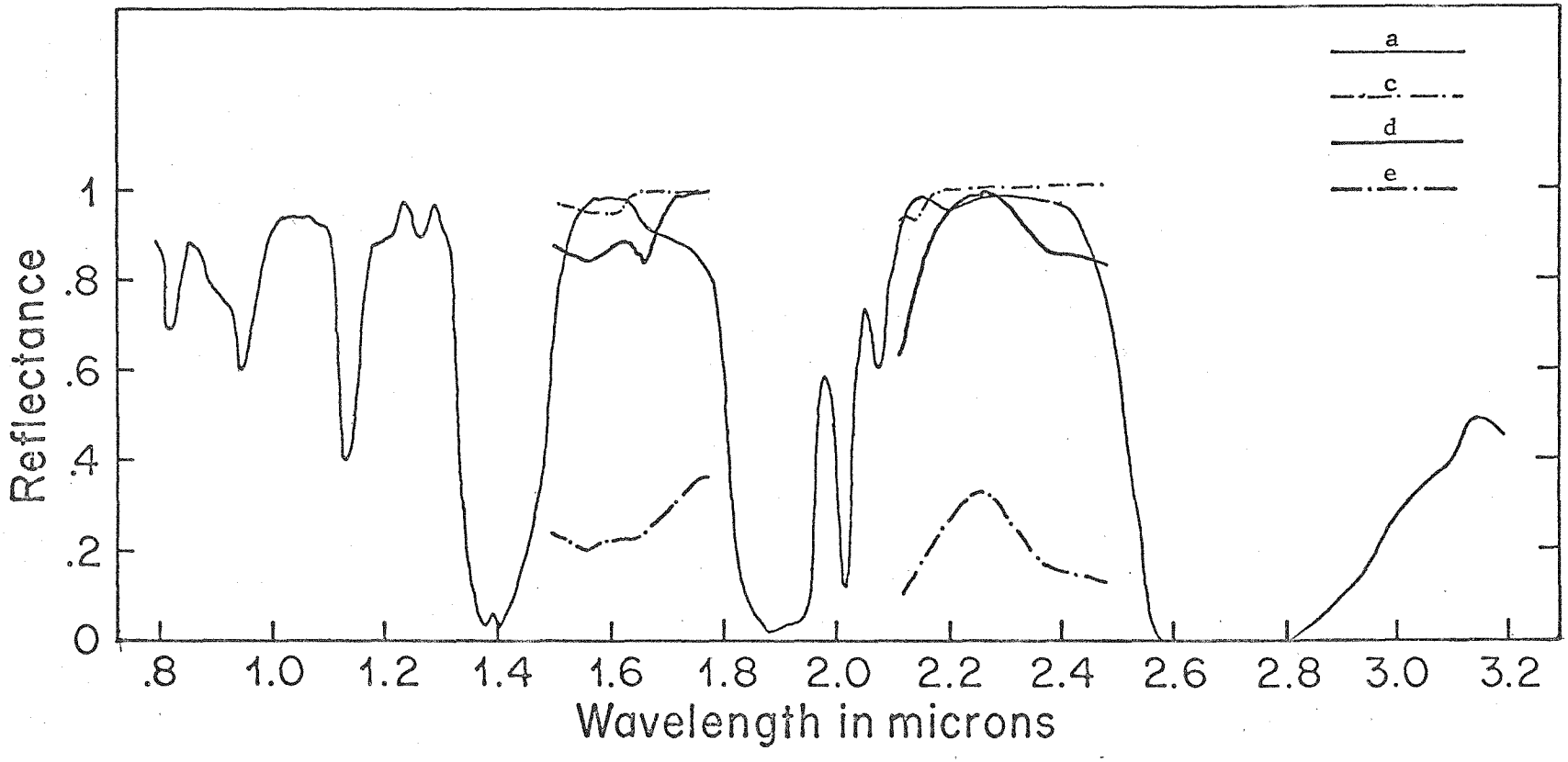

Figure 15. Spectral reflectance of pure CO_2 and H_2O frosts compared with the transmittance of the terrestrial atmosphere . (a) Transmittance of the terrestrial atmosphere during typical dry conditions. (c) Very coarse-grained CO_2 frost. (d) and (e). Very fine and medium-grained H_2O frosts.

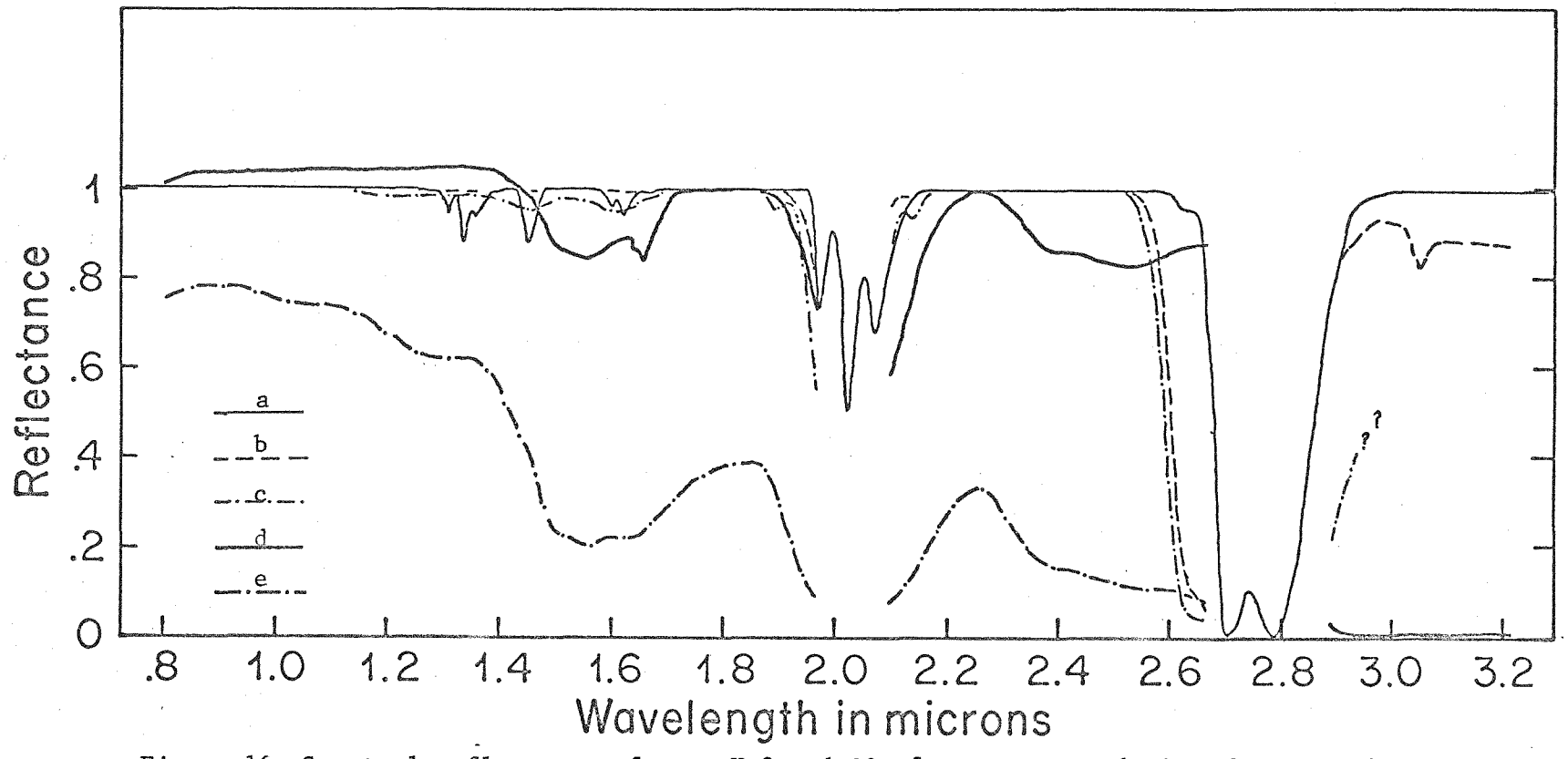

Figure 16. Spectral reflectance of pure H_2O and CO_2 frosts compared with the transmittance of the Martian atmosphere. (a) Transmittance of the Martian atmosphere (100 m-atm. CO_2 at 0.01 atm. and 250°K) . (b) and (c). Fine and very coarse CO_2 frosts. (d) and (e). Fine and medium grained H_2O frosts.

FIGURE CAPTIONS

Figure 10. (a) Photograph of a 3 mm thick, fractured layer of CO_2 on the bottom of the chamber. This sample is not optically thick. Actual size. (Spectrum 2c.)

(b) Photomicrograph of the surface of a fine-grained pure CO_2 frost. The coarse texture (1/2 mm) corresponds to the scale of the columnar structure of the interior of the deposit. The fine surface texture (10-20 microns) largely controls the reflection spectra. x40. (Spectrum 8a).

(c) Photomicrograph of a cross section of a very fine-grained H_2O frost deposit. Grain size is less than 10 microns. Deposit is 0.3 mm thick (0.004 g/cm^2). Density is 0.015. x40. (Spectrum 4a).

(d) Photomicrograph of the bulk material from a fine-grained H_2O frost. Grain size is about 30 microns, but fine texture exists below the resolution (5 microns). x40. (Spectrum 4b).

Figure 11. (a) Photomicrograph of a fragment from a coarse-grained 5% H_2O-95% CO_2 frost. The vertical columnar texture is typical of predominately CO_2 frosts. Grain size 100 x 1000 microns. x40. (Spectrum 6c).

(b) Photomicrograph of disaggregated grains from the same frost as shown in Fig. 11a. The columnar grains extend through the deposit. The conical points on the bottom of the grains are typical of coarse-grained, predominately CO_2 frosts. Grain size 100 x 1000 microns, but surface texture scale is 20 microns. x40. (Spectrum 6c).

(c) Photomicrograph of the bulk material from a fine-grained 10%H_2O-90%CO_2 frost. Grain clumps about 80 microns in diameter. Fine texture at about

10 microns governs scattering. x 40. (Spectrum 7a).

(d) Photomicrograph looking directly at the surface of a very fine-grained 23% H_2O - 77% CO_2 frost. Grain size 10 microns. The smaller specular reflections indicate that scattering occurs also on this scale. x 40. (Spectrum 7d).

Figure 12. (a) Photograph of the cross section of a dense coarse-grained 20% H_2O-80% CO_2 frost showing strong columner texture. x 6. (Spectrum 7c).

(b) Photomicrograph looking directly down on the surface of the same frost as shown in Figure 12a. Grain cross section is about 1 x 1 mm. Little scattering occurs on a finer scale. x 25. (Spectrum 7c).

(c) Photomicrograph of the interior of the same frost as shown in Figure 12a. Grain size about 0.6 x 2.5 mm. Scattering occurs on a 100-200 micron scale. x 25. (Spectrum 7c).

(d) Photomicrograph of the interior of a frost with all texture at one scale (100 microns). This was uncommon among the laboratory deposits. x 40.

APPENDIX I

INSTRUMENTATION

A LOW ENERGY SPECTRAL REFLECTOMETER FOR FROSTS

ABSTRACT

A low incident energy, near infrared spectral reflectometer has been designed and built as an integral part of an environmental chamber used for the growth and observation of frosts. The incident energy required for spectral measurement, 10^{-6} watts-cm^{-2}, is five orders of magnitude less than that used in previous measurements of frosts and avoids metamorphism of the sample. Simple, readily interchangeable chambers are used, permitting growth of samples under a variety of controlled conditions and spectral measurements over a wide range of inclinations.

INTRODUCTION

Frost deposits are intrinsically difficult to observe or measure without altering their texture or composition. In particular, they must be kept cold and isolated from atmospheric condensation. This paper describes apparatus used to grow frost deposits under controlled conditions and measure their reflectance spectra without altering the samples.

Spectral reflectance measurements of frosts made previously (Keegan and Weidner, 1966; Zander, 1966) were of samples illuminated directly with a globar or similar infrared source. The radiant fluxes used in those studies were not stated, but are estimated from the description of the equipment to have been about 0.1 watt-cm^{-2}. Such flux levels, corresponding to black body radiation of 90° C, are large compared to the radiation at typical frost temperatures and can result in significant alteration of frost specimens. However, by projecting onto the sample only a chopped, monochromatic beam, and using synchronous detection techniques, the incident flux level can be greatly reduced. The equipment described herein uses this method and requires an incident flux level of only 3×10^{-6} watts-cm^{-2} for a detection signal-to-noise ratio of 1500 with a 0.35 second time constant.

The frosts were grown from pure gases at low temperature and pressure in a simple, versatile environmental chamber. The frost composition and growth rates were controlled by accurate regulation of the gas flow rates. The experimental apparatus used in the growth of frosts and measurement of their reflection spectra is shown schematically in Fig. 1. This apparatus has been used to obtain reflectance spectra of a wide variety of carbon dioxide and water frosts from 0.8 to 3.2 microns.

GROWTH OF FROST SAMPLES

Frost samples were grown by allowing a regulated flow of condensible gas into a large chamber whose lower portion was immersed in a coolant. The chamber consisted of a stainless steel beaker (Volrath 8-liter) seated against an O-ring in a thick aluminum lid.

Several variations of the plain stainless steel beakers were used. One chamber was painted on the inside with a flat black epoxy paint (Cat-a-lac Flat Black) and this was used for most of the measurements. The center bottom of one beaker was replaced with a truncated stainless steel cone onto which different forms of heat sinks could be attached. Samples grown on a plate resting on the smooth, flat interior surface of this cone could be raised to different angles to measure inclined reflectance at constant phase angle.

The chamber lid contained all the windows, electrical and mechanical feedthroughs and connections to the gas system. All apparatus inside the chamber, except the inclined stage, was attached to the chamber lid so that beakers could be exchanged readily. A low wattage lamp inside the chamber allowed visual observation and photography of the frost through an auxilliary window.

The two main components of the gas system were: (1) a mixing manifold which was connected through shut-off and regulating valves to the source gases and a mercury manometer and (2) a main manifold which was connected through shut-off valves to the chamber, mixing manifold, McLeod gauge, thermocouple gauges and a liquid nitrogen cold trap. A small vacuum pump was connected to the cold trap and exhausted outside the laboratory to avoid oil contamination on the infrared optics and filters.

Normally, the chamber was filled and evacuated through the main inlet.

An expansion cone was used on this inlet to help make the frost deposit uniform across the bottom of the chamber. In order to be able to transfer water vapor into the chamber when the chamber pressure was greater than the vapor pressure of water at room temperature (20 torr) without the use of a boiler, an auxiliary system was used. Gas was bubbled through distilled water and the resulting saturated vapor was fed into the chamber through the auxiliary inlet.

The uniformity of the deposit depended on the condensible gas flow rates, total chamber pressure, shape of the inlet, and good contact between the chamber and the coolant. Normally no difficulties were encountered and the frost was visually uniform across the entire bottom of the chamber. The final procedure was the result of some experimentation. Uniformity could be achieved over a reasonable range of flow rates and pressures. However, increasing the flow rate or decreasing the pressure from this range would yield a relatively thicker, coarser deposit directly under the inlet. Decreasing the flow rate or increasing the pressure from this range would result in most deposition occurring high on the chamber wall with a thin deposit on the chamber bottom. As the saturation temperature of H_2O is considerably higher than that of CO_2, there was some fractionation of mixed samples. The composition of the area viewed by the detector was determined by collecting a sample from this area and weighing it accurately as it was allowed to warm up.

When there were noticeable gas velocities in the chamber, a quiet boundary layer could sometimes be observed as the location of a thin "cloud". Attempts to get most of the crystals to form in suspension were not successful.

Temperature control and heat budget

The chamber was cooled by immersion in a liquid bath, usually liquid

nitrogen (77°K). The chamber was tilted slightly to prevent trapping of gas under the center of the chamber bottom. Even at the high frost growth rates, the temperature at the inside of the chamber wall was within one degree of the fluid temperature.

Two other liquid coolant systems were used to attain intermediate temperatures in the chamber: Freon 11 (Trichlorofluoromethane, freezing point 162°K) and n-propyl alcohol, (freezing point 146°K). Freon, though difficult to handle (its ambient vapor pressure is just 1 atmosphere; it dissolves styrofoam readily) has a high latent heat and low viscosity at its freezing point. All alcohols have extremely high viscosities near their freezing points and cannot be circulated. These liquids were cooled by circulating liquid nitrogen through the cooling coils immersed in them. The temperatures of the chamber and the liquid were monitered with thermocouples. The chamber lid was not insulated above and usually attained a temperature slightly above 0°C.

The heat and radiation loads on the sample are listed in Table 1 along with some comparison values. The amount of radiation absorbed by the sample depended on its reflectance. During sample growth, heat sources other than the latent heat release were minor. The radiation from the monochrometer was completely negligible at all times. More than 90% of the heat load on the sample was removed by conduction to the chamber walls.

Sample purity

The following is a list of the gases used in the experiments:

Carbon dioxide: J. T. Baker Instrument grade.

Maximum total impurities	100 ppm
H_2O	30 "
N_2	70 "
O_2	25 "
H_2	15 "
CH_4	15 "

Water vapor: Vapor over triply distilled water at ambient temperature in a glass boiling flask. The water was pumped down to the ambient boiling point after being connected to the system.

Nitrogen: J. T. Baker Prepurified.

Maximum total impurities	30 ppm
Typical dew point -85° F	4 ppm
Typical oxygen content	8 ppm

The source cylinders were connected to the manifold with small diameter tygon tubing. To minimize contamination by gases diffusing through the tubing walls, these lines were evacuated prior to each run by closing the valves on the cylinder regulators and pumping the manifolds and flexible lines down to less than 100 microns. The lines to the water source were cleared by pumping for a minimum time of about one minute after the pressure had reached its minimum. All small flexible lines except the water vapor line were normally kept at atmospheric pressure or greater, so that total pressure gradients were not set up through the tubing walls.

The total leakage and outgassing diffusion rate into the mixing and main manifolds was measured to be 0.09 liter-microns sec^{-1}. The total leak and outgassing rate of the chamber alone was measured to be 0.012 liter-microns sec^{-1}.

The small amount of H_2O in the CO_2 source gas was sufficient to cause major spectral changes near 3.1 microns. To obtain nearly pure CO_2 frosts, a cold trap consisting of 8 feet of 1/4" copper tubing at dry ice temperature was put in the CO_2 gas line. Assuming that the H_2O partial pressure was reduced to its equilibrium value in this trap, the resulting H_2O concentration was 0.8 ppm. This process eliminated most or all of the effects of H_2O contamination.

Measurement of spectral reflectance

The spectral reflectometer consisted of a filter monochrometer mounted above the chamber, a detector and movable standard surface inside the chamber, and associated electronics.

The filter monochrometer consisted of a quartz envelope tungsten lamp, a spherical first surface condensing mirror, a multibladed, rotating chopper (30 Hz) with phase detector, and a set of "plug in" filter wheel modules. The filter wheel modules contained the slits, a disk of discrete filters or a continuously variable filter wheel, and the filter wheel drive and punch command unit. They could be interchanged in a few seconds.

Module A was a continuously variable filter wheel (Optical Coatings Laboratory) covering the range from 1.58 to 3.2 microns in half a revolution. Its half-peak band width was less than 2% of the center wavelength. The peak transmission varied from 10% at 1.6 microns to a maximum of 40% at 2.9 microns. The B module contained eight discrete filters (Thin Films, Inc.) from 0.8 to 1.5 microns. The C module contained 18 filters (Optics Technology) spaced uniformly in wavelength from .8 to 1.65 microns. The transmission characteristics of the

B and C filter sets are given in Table 2. A spring loaded dark slide rested against the module and swung into the beam as the module was removed.

The monochrometer projected diverging, chopped unpolarized radiation onto the central portion of the chamber bottom through a calcium fluoride window. The upper surface of this window was bathed in argon to prevent water condensation in the beam path. An area approximately 3" in diameter was illuminated on the chamber bottom. The central 3/4 inch square of this area was viewed by a lead sulfide detector-field lens assembly attached to the chamber lid. The detector was a 2 mm x 2 mm photoconductive ambient lead sulfide cell mounted on a quartz substrate with a sealed quartz cover slip (Santa Barbara Research Corp.). The 1 inch focal length f: 1 Irtran 2 field lens was heated with an edge-wound coil to prevent frost formation. Powder blasted gold, powder blasted silver, brushed aluminum and smoked magnesium oxide were used as reference surfaces. A diffuse reflecting reference surface mounted on an arm attached to the lid could be lowered to hang just above the center of the chamber bottom and parallel to it. When the reference arm was in the raised position, the reference surface fitted snugly against a heater coil to prevent any frost formation on this surface.

The signal from the detector was amplified by a low-noise operational amplifier mounted immediately outside the chamber. This signal was fed to a low noise, high-gain amplifier where it was correlated with the output of the phase detector. The resulting dc signal was recorded on a strip chart recorder and by a digital voltmeter - paper tape punch for later processing by the computer.

Reflectance spectra of frosts samples were obtained by measuring the reflected intensity from the sample and the reference surfaces successively.

The dark level was recorded before each scan and subtracted from all measurements. The ratio of these two scans is the spectrum of the sample compared to the spectrum of the reference surface, and is independent of all geometric factors and the spectral properties of all elements of the system which do not change in the brief period required to make the two scans. The only element whose spectral properties had to be kept constant was the reference surface. Between two scans there could be small changes of the water vapor content along the light path in the monochrometer. This could be detected only in the 2.7 micron band where, of course, the earth's atmosphere is completely opaque. In practice, this variation was not noticeable. The major sources of error were variations of the source intensity and long period drift of the detector sensitivity. These limited accuracy to about 1%.

APPENDIX II

DETAILED PROCEDURE

DESCRIPTION OF A STANDARD RUN SEQUENCE

1. The chamber was closed and pumped down to less than 40×10^{-3} torr with the reference lowered.
2. The chamber inlet was closed, the reference raised, lens and reference heaters turned on, calcium fluoride window cleaned, and argon flow started in the window shield.
3. The liquid nitrogen flow was started.
4. If the water source was to be used, it was pumped on to purge out any other gases.
5. With the water vapor source and chamber valved off, the rest of the gas system and flexible lines were pumped down with the metering valves full open.
6. When the chamber was cold, the buffer gas was added and the chamber pressure measured.
7. The electronics were turned on to warm up. The source lamp voltage and amplifier time constant were set.
8. The buffer gas pressure was measured cold. The metering valves were set.
9. Condensible gas flow was started. The reflectance of the chamber bottom was monitered (usually at 2.2 μ).
10. During growth, the frost deposit was checked visually (preamp off, chamber lamp on) at least once to ascertain if the deposit was uniform.
11. To make a spectral recording, the gas flow was turned off and the gain of the amplifier set. A scan was made of the sample. The reference was lowered and a scan made of the reference. The filter module was changed and another scan made of the reference. The reference was raised and a scan made of the sample.

12. The non-condensible gas pressure could be measured at this time.
13. Steps 9 and 11 were repeated if desired.
14. The sample was photographed through the chamber windows.
15. When growth was completed, the chamber pressure was raised to atmospheric with dry nitrogen. A small positive flow of dry nitrogen was maintained into the chamber until the sampling for weighing and photomicrography w completed.
16. A sample of frost was taken from the center of the chamber for weighing to determine composition.
17. Samples of the frost were transferred to the cold stage for photomicrographs.
18. The cold dewar was removed. The cold chamber was removed, a clean, warm chamber put in place and evacuation started quickly to minimize contact of the reference surface with the atmosphere and to minimize frost formation on the apparatus attached under the lid. The apparatus was allowed to warm up while the vacuum pump was connected.
19. When not in active use, the chamber was normally stored either under vacuum and being pumped on, or was filled with one atmosphere pressure of dry nitrogen.

COMPOSITION DETERMINATION

The H_2O/ CO_2 ratio was determined by isolating the sample and weighing it continuously as it was allowed to warm up. The initial rapid loss of weight reflected the sublimation of CO_2. It is assumed that the amount of H_2O versus CO_2 lost in this period was not greater than the ratio of their vapor pressures (10^{-6}). The formation of liquid indicated that the remaining sample was water.

The primary difficulty encountered was the formation of water frost on the cold vial. Eventually a procedure was adopted wherein the sample was transferred to the balance in a double vial inside a small dewar. First the inner lucite and the outer brass vial were both cooled in liquid nitrogen, assembled together and transferred into the chamber through one of the window ports. The vials were opened, a section of frost placed in the inner vial, and the pair reassembled by manipulation with long handled tongs and scoops through the port. The vials were placed immediately in a small dewar and transferred to the balance room. The air in the balance was kept dry with four wire mesh columns of magnesium perclorate. The vial pair was placed in the balance through a small opening, the inner vial extracted and placed on the pan. By this procedure, the addition of significant water frost to the sample or weighing vial was avoided.

Five mg. of water could easily be seen inside the vial. It is estimated that 0.5 mg. could have been noticed on the outside of the vial. The precision of the weighing was somewhat better than this. With a typical initial sample weight of 1 gram, the H_2O weight fraction could be determined with an accuracy of 0.001 or 10% of its value, whichever was greater.

SAMPLE PHOTOMICROGRAPHY

Samples of the frost deposit were transferred in a stainless steel scoop and small dewar to a cold stage in a larger dewar designed for photography. Sample deterioration could be readily identified by the formation of a characteristic water frost on its surface. To circumvent this problem, the samples could be broken open to expose fresh surfaces after they were transferred onto the cold stage. The cold stage had sufficiently poor insulation so that boiling of the liquid

nitrogen pool in the bottom of the dewar created a moderate outflow of dry gas from the stage. Microscope objectives (42 mm and 29 mm focal lengths) mounted on long extensions were the only optics used, and gave photographic negative scales of seven to ten times actual size. The surface of the frost deposits were also successfully photographed in situ with the same optics.

MEASUREMENT OF THERMAL CONDUCTIVITY

The thermal conductivity of the frost deposit could be measured in situ. When sample growth finished, the buffer gas was pumped out. With the chamber pressure approximately 40 microns, $C0_2$ was let in at a calibrated rate. The pressure rise was monitered with the thermocouple gauge mounted in the chamber lid. The $C0_2$ rate was chosen so that the pressure rise was about 50 microns, keeping the pressure in the range where thermocouple gauges are most sensitive. At these pressures, the impedence of the chamber to gas flow is negligible and the pressure at the lid can be assumed to equal that at the frost. This pressure rise thus represents the change in saturation pressure of the frost surface, and can be equated to the temperature of the frost surface. The heat load could be calculated directly from the $C0_2$ flow rate, and the thickness of the frost deposit measured when the chamber was opened. The temperature at the base of the frost was assumed to be equal to the chamber wall temperature. The saturation temperature-pressure relation is so sensitive to temperature that the frost surface temperature could be determined quite accurately in this fashion. The computed conductivity is an average for the entire thickness of the frost. Comparison of photomicrographs of samples subjected to this process with those of normal samples did not indicate any appreciable densification of the initial deposit. The $C0_2$

added in the conductivity measurements appeared to form a dense layer on the surface of the initial deposit.

APPENDIX III

FROST EMISSIVITY AND RADIATION BALANCE OVER THE MARTIAN POLAR CAP

Emissivity of frost deposits

It has previously been assumed that frozen CO_2 will have emissivity near one and that the radiative loss from CO_2 frost on Mars is limited by blocking by the 15 micron CO_2 gas band (Leighton and Murray, 1966) and the formation of H_2O ice clouds (Leovy, 1966). However, the spectral emissivity of a fine-grained frost will be low outside of absorption bands. The effective emissivity of such a frost through a thick atmosphere which had absorption bands at the same wavelengths would be small. This is the situation of CO_2 frost on Mars.

Two possible models of frost scattering are Lambert's law and the law of diffuse reflectance for isotropic scattering. Lambert's law is the simplest model of scattering. In principle, isotropic scattering theory allows calculation of the reflectance and emissivity of a particulate scattering medium from textural information and the optical properties of the bulk solid. In practice, exact calculations are difficult and probably not warranted unless the scattering phase law can be shown to be exactly isotropic, which cannot be done for frosts. However, the emissivity of a scattering medium can be directly related to its normal reflectance. This relation is quite useful. For isotropic scattering of monochromatic light, the single parameter describing the medium is the albedo for single scattering ϖ. This is the ratio of the probability of scattering to the probability of scattering plus absorption.

Lambert's law is

$$I_{(\mu)} = r_0 F \mu_0$$

and the law of diffuse reflection for isotropic scattering is

$$I_{(0,\mu,\mu_0)} = \frac{1}{4} \varpi F \frac{\mu_0}{\mu+\mu_0} H_{(\mu,\varpi)} H_{(\mu_0,\varpi)}$$

(Chandrasekhar, 1960, p. 85) where

I = reflected intensity

πF = incident flux

r_o = normal backscatter reflectance

ω = albedo for single scattering

H = isotropic H-functions

μ = cosine of the angle of reflection

μ_o = cosine of the angle of incidence

The equivalent to r_o for diffuse isotropic reflectance (normalized to I maximum) is

$$\frac{\omega H^2(1,\omega)}{H^2(1,1)}$$

The emissivity of a surface obeying Lambert's law is simply $1 - r_o$. The emissivity of an isotropic scattering medium is

$$2\sqrt{1-\omega}\int_0^1 \mu H(\mu,\omega)\,d\mu$$

The reflectance increases and the emissivity decreases very rapidly as ω approaches unity. This relation is shown in Figure 2. The sum of the normal backscatter and emissivity is always 0.9 or greater.

One test of the degree to which frosts obey these basic scattering laws has been made in the laboratory by measuring the spectral reflectance for backscatter at different inclinations. These measurements showed the laboratory frost to be more nearly Lambert than diffuse. This suggests that the emissivity of a frost can be approximated by one minus its reflectance for normal incidence and reflection. The reflectance of a frost will be high if the mean path length through the particles (grain size) is much less than the inverse of the absorption coefficient and greater than the radiation wavelength.

The preceding discussion, combined with the laboratory reflection spectra and gas absorption spectra at longer wavelengths, indicates that the spectral emissivity of a CO_2 frost will be low outside of the strongest absorption bands for a grain size range of 40 microns to at least 3 mm.

The rate of heat loss from the surface depends on the emissivity of the deposits convolved with the transmission of the atmosphere. Here there is a significant difference between water and carbon dioxide frost on Mars. The only abundant infrared active constituent of the Martian atmosphere is carbon dioxide, which does not have a pure rotation spectrum. For blackbody radiation of temperatures of 150° to 200° K, the only strong atmospheric absorption band will be the 15 micron CO_2 band. The effective emissivity of a scattering CO_2 frost through a CO_2 atmosphere may be especially poor as there is no significant shift in frequency between the CO_2 gas and solid vibration lines. However, the libration fine structure in solid CO_2 is not resolved, so that CO_2 frost would be able to radiate between the gas rotation lines where they were not saturated. CO_2 frost radiative loss would then be primarily by radiation between the gas rotation fine structure, radiation on the wings of the absorption bands where the atmosphere was not opaque (but the frost emissivity was appreciable), and radiative coupling with the atmosphere in the 15 micron band. Radiative transfer within the Martian atmosphere by CO_2 absorption bands has been discussed by Goody and Belton (1967) and Gierasch and Goody (1967).

Water ice has a strong vibration-libration and pure libration spectrum and would be able to radiate to space well in regions other than the 15 micron band of CO_2. Hence, under cloudless Martian polar conditions, water frost would be able to lose heat readily by radiation.

From 15 to 88 microns, no CO_2 absorption features are known or expected other than the wings of the ν_2 and lattice vibration bands. This interval contains 85% of the blackbody radiation at 150°K. Measurement of the spectral emissivity of solid CO_2 in this region is imperative to the study of the radiation balance of a CO_2 frost under a CO_2 atmosphere. If the assumption of Lambert or isotropic scattering holds at longer wavelength (to 50 microns) the spectral emissivity of CO_2 frost could be determined by measurement of its reflection spectra, which, at the low temperatures necessary, is a considerably easier experimental problem than direct measurement of spectral emissivity.

The effect of clouds on the radiation balance

Recurrent clouds over the polar cap (the "polar hood") have been reported by many observers (see Capen, 1966). The formation of CO_2 clouds can only decrease the outward net radiation flux. H_2O crystal clouds, by increasing the amount of water in the atmosphere, might appreciably increase the outward net radiation from the cloud level. The reported absorption coefficient of H_2O for low temperature radiation (1500 g^{-1}, Cunningham et al., 1963; 7000 g^{-1}, Caren et al., 1963) is on the order of 100 times that reported for CO_2 (8 g^{-1}, Caren et al., 1963; 50 g^{-1}, Cunningham et al., 1962). Saturation of the 15 micron CO_2 band will decrease the effective absorption coefficient of CO_2.

Since the emissivity of small grains is proportional to the absorption coefficient, this suggests that if the atmosphere is at the CO_2 saturation pressure any water clouds would become regions of CO_2 condensation. A distinct possibility is that the H_2O crystals would be the actual site of CO_2 condensation, and that this CO_2 coating would grow until it became opaque to the radiation from the H_2O core or until the flake fell as snow. Leighton (personal comm., 1967) has suggested

that high level snow formation and subsequent sublimation at low or ground level could be an effective heat transport process in the Martian atmosphere. The details of cloud formation and snowfall merit further investigation, but are beyond the scope of this thesis.

APPENDIX IV

SPECTRAL AND PHYSICAL PROPERTIES OF H_2O AND CO_2

Spectral and Physical Properties of CO_2 and H_2O

Major differences between CO_2 and H_2O relevant to Martian frosts are the latent heat of sublimation and the saturated vapor pressure-temperature relations. The saturated vapor curves for CO_2, H_2O and some other gases are shown in Figure 3. Some physical properties of H_2O, CO_2, and N_2 are presented in Table 3.

The spectral properties of H_2O vapor, liquid, bulk solid and natural clouds have been studied extensively. Nearly all spectral studies of CO_2 have been of the gas or of the transmission spectra of solid thin films at 15 microns and longer wavelengths. Some of this literature is reviewed below.

H_2O Spectra

The absorption of water vapor has been discussed extensively by Goody (1964) and computations of its spectral transmittance from one to ten microns have been made byWyatt, Stull and Plass (1964). These data are summarized in Fig. 4.

The infrared spectrum of ice has been reviewed by Ockman (1958). The fundamental vibrations are shifted from those of the gas due to changing of the O-H bond length. The frequency of the ν_1 and ν_3 modes of ice are very close to twice that of ν_2; hence the harmonics are closely grouped.

At least three modifications of Ice I exist at low temperatures: hexagonal, cubic and vitrious. Small temperature effects on the frequency of some modes have been reported (White, 1952; Ockman, 1958; Zimmerman and Pimentel, 1962).

There is some disagreement on whether spectral differences between hexagonal and cubic Ice I exist (White, 1952; Ockman; 1958) or not (Bertie and Walley, 1964).

Recent spectral reflection measurements of natural clouds covering the 1-2.5 micron region (McDonald and Deltenre, 1963; Blau et al, 1966) have not been corrected for the solar spectrum and are not readily reducible to ice reflection spectra. Spectral reflectance of cirrus and cumulus clouds have been measured by Blau et al. (1966) over the 1.2 - 2.4 micron region with spectral resolution of about 1/50. Cumulus clouds (liquid water) showed pronounced minima at 1.39 and 1.90 microns. Cirrus clouds (ice) had minima at 1.47 and 1.97 microns. The spectral scattering of laboratory ice clouds and frost from 1.0 to 8.0 microns has been measured by Zander (1966). Clouds and frosts had similar reflection spectra except for a small sharp maximum at 2.6 microns in the cloud spectrum.

The reflection spectrum of a smooth, polycrystaline ice block was measured from 2.5 to 5.0 microns by Alkezweeny and Hobbs (1966). Their results show a stronger reflection at the 3.1 maximum (45%) than Zander obtained for frosts. Liquid water reflection spectra have minima at 2.75, 5.8 and 10.9 microns and maxima at 3.1, 6.2 and 14.3 microns (McSwain and Bernstein, 1961).

CO_2 spectra.

The absorption spectrum of carbon dioxide gas is discussed by Goody (1964) and computations of its spectral transmittance from one to eighteen microns have been made by Stull, Wyatt, and Plass (1964). These data are summarized in Figure 4. More detailed measurements of the absorption of the

major infrared bands were made by Burch, Gryvnak, and Williams (1962). In the near infrared, transmission spectra of solid CO_2 show frequency shifts of the fundamentals of less than 10 cm^{-1} from the gas fundamentals (Osberg and Hornig, 1952).

CO_2 lattice vibrations were first observed in combination with the fundamentals. The derived lattice frequencies were 63 to 126 cm^{-1} (Jacox and Milligan, 1961). The lattice vibrations have now been observed directly at 68 and 114 cm^{-1} (Ron and Schnepp, 1967; Anderson and Walmsley, 1964; Anderson and Gebbie, 1965). CO_2 is a symmetric molecule and has no pure rotation spectrum. No absorption features are known or expected between the 15 micron band and the lattice vibrations at 88 microns.

The only previous reflection spectra of CO_2 frost were obtained by Keegen and Weidner (1966) who measured samples of liquid water, H_2O frost, CO_2 frost, and crushed commercial dry ice from 2.5 to 20 microns. Unfortunately their CO_2 samples appeared to have been badly contaminated with at least H_2O .

APPENDIX V

ORIGINAL STATEMENTS OF

KUIPER, MOROZ AND DOLLFUS

From Kuiper, 1952 (p. 361):

Infrared reflection spectra were obtained of snow, both fresh and melting. It was found that these spectra resemble that of a transmission spectrum of a water cell of specific thickness. Fresh snow near 0° C is equivalent to about 10 mm of water; melting snow in surroundings of 10° C to about 20 mm. Evidently the light-path within the snow depends on the size and shape of the ice crystals. Very fine crystals return the light after a short path-length. In fact, laboratory experiments with H_2O frost deposits on dry ice (-78° C) showed a water-cell equivalent of only 1 mm.

The observations of the Mars polar cap showed that the cap resembles a water-cell spectrum with about 1 mm equivalent path. These observations were difficult because of the small extension of the polar cap (about 2 square seconds of arc) and the low-intensity level, but they were repeated several dozen times with consistent results. In these observations the two large flint prisms of the spectrometer were replaced by a single 25° quartz prism, which reduced the resolution to only 9 but increased the sensitivity about twenty-five times. This adaptation brought the solution of the polar-cap problem just within reach.

Laboratory tests with CO_2 snow showed this substance to remain "white" up to 2.5μ except for three shallow absorptions near 2μ corresponding to the strong CO_2 gas absorptions. Terrestrial snow is nearly black beyond 1.5μ and almost fully black beyond 2.0μ. Cold frost, as found on Mars, behaves similarly, though the drop at 1.5μ is less steep.

The conclusion is that the Mars polar caps are not composed of CO_2 and are almost certainly composed of H_2O frost at low temperature (much below 0° C).

From Moroz, 1964 (p. 279):

On the night of March 16-17 [1963] observations of the polar cap spectrum were made in the region of 1-2μ. The observations were made with a 2 mm exit slit, giving a resolution of $\Delta\lambda \simeq 1800$ Å at 1.6μ. The width of the entrance slit was 0.15 mm and the height was 0.3 mm. The slit was oriented at a tangent to the planetary disk in the polar region. The recordings of the polar region sometimes differed greatly from one another due to vibration of the disk and errors in guiding, but if obviously defective cases are rejected, on an average they show a definite difference from recordings at the center. The interval 1.5 - 1.8μ in the polar cap spectrum is characterized by a lesser intensity than in the spectrum of the central region, and, in addition, the absorption band at 1.5μ in the polar cap spectrum is displaced in the direction of long waves. Both these peculiarities are characteristic of the spectrum of reflection of ice, snow and frost (for example, see (7)). Kuiper (2) already has noted the presence of these peculiarities in polar cap spectra. The polar caps apparently consist of frozen water. A similar conclusion was drawn by Dollfus (28) from observations of a completely different type (polarization curve of the polar cap).

(2) G. P. Kuiper, (1952)

(7) V. I. Moroz, Astron. Zh., 38, 1080, (1961)

(28) A. Dollfus (1961)

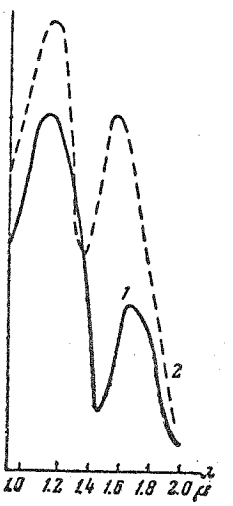

Moroz Figure 6.

Fig. 6. Spectra of polar cap (1) and center of Martian disk (2) in 1-2μ region. Prism spectrometer, PbS, with CO_2 cooling, mean of three recordings, entrance slit 0.15 x 0.3 mm, exit slit 2 mm ($\Delta\lambda$ = 1700 A at 1.5μ), rate 70 Å/sec, τ = 2.2 sec.

From Dollfus, 1961 (p. 381):

The polar caps are quite small and difficult to measure. They are often covered by clouds or light veils and should be observed only with the Martian atmosphere clear. Nevertheless, it has been possible to make a number of measures during the spring regression, shown by circles in Figure 33. The polarization of the polar material remains very small and variable during that season for all phase angles. Ice, hoarfrost, and snow deposited on mountains show, when melting and refreezing, strong positive polarization, if seen at the phase angles used to observe the Martian poles. This polarization comes from the light reflected in the interior of the ice and refracted with a plane of vibration normal to the plane of vision.

Fresh snow also shows positive polarization, though less than melting snow. Polarization in natural or artificial hoarfrost, deposited in small crystals in the laboratory at normal atmospheric pressure, is also higher than in the Martian deposits. However, the atmospheric pressure on Mars is only one-tenth of that on the earth. Hoarfrost formed under these conditions is found to consist of smaller grains. When heated by an electric arc, the hoarfrost sublimates without melting, and the remainder takes on the appearance of opal glass, full of small pores and cavities. In the process the albedo is reduced, and the polarization becomes very similar to that of the Martian polar caps. In Figure 33 the crosses refer to sublimating hoarfrost and are seen to agree remarkably well with the circles representing the Martian polar caps. It thus seems probable that the white spots at the poles of Mars are a deposit of hoarfrost which sublimates under the sun's radiation.

The edges of the polar caps show bright local spots. The light from these is polarized differently. The minimum at $V = 14^{\circ}$ has the exceptional negative

value of -0.022. No laboratory source has shown such values, but clouds of ice crystals show exactly this phenomenon. Visual observations show that these spots are located where the polar deposits last longest, presumably elevated areas. These spots would then be due to material evaporated from the polar cap, recondensed locally because of higher elevation of the ground.

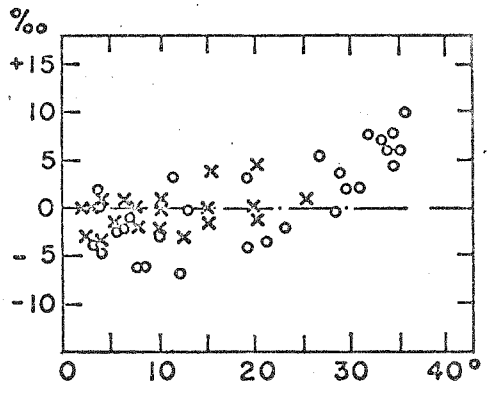

Dollfus Figure 33.

Fig. 33 -- Mars, polarization (unit 0.001) of polar cap in spring. Open circles: polar cap; crosses: laboratory deposit of hoarfrost, sublimating under 80-millibar pressure.

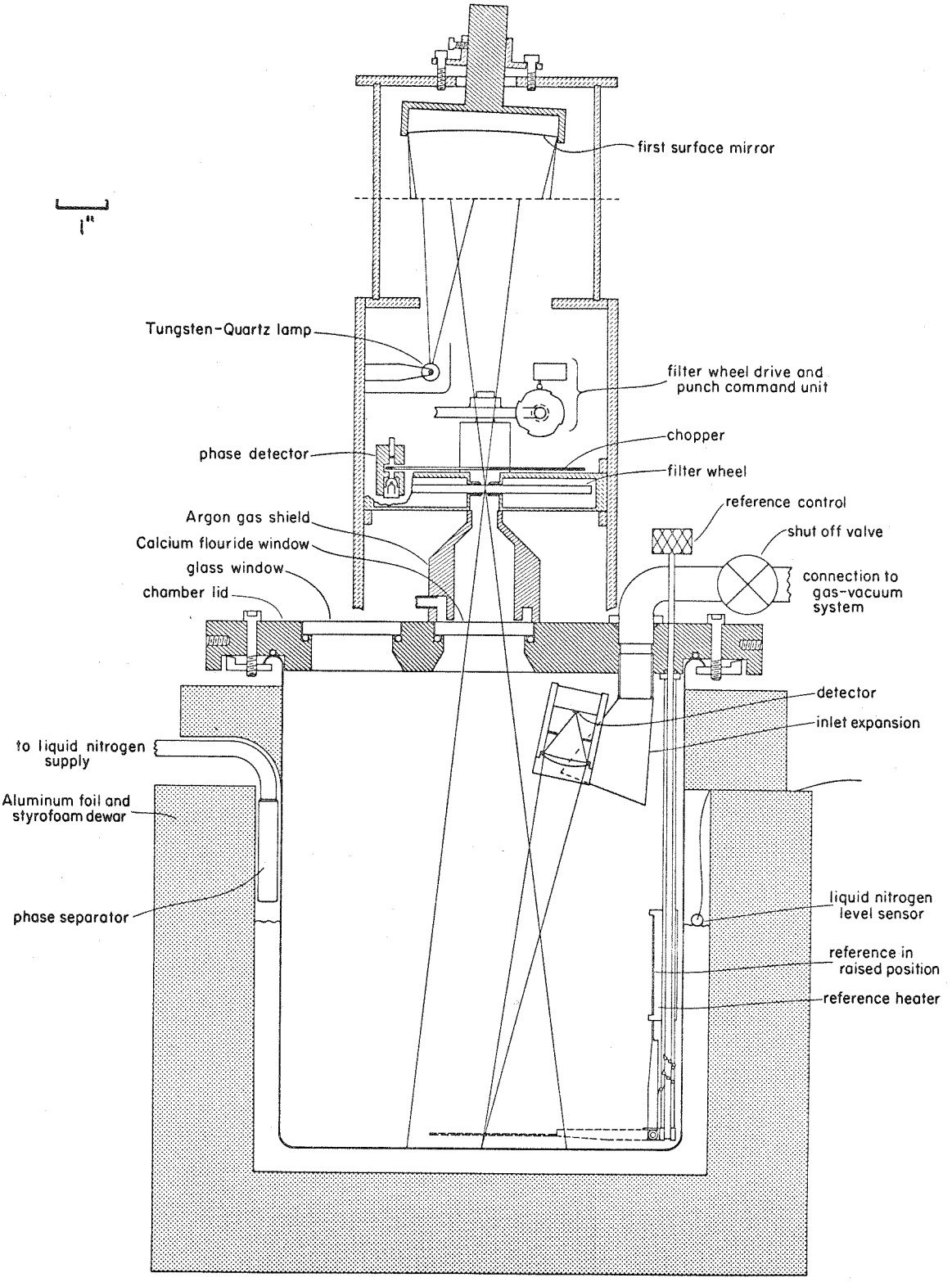
1"
first surface mirror
Tungsten-Quartz lamp
filter wheel drive and punch command unit
chopper
phase detector
filter wheel
reference control
Argon gas shield
shut off valve
Calcium flouride window
glass window
connection to gas-vacuum system
chamber lid
detector
inlet expansion
to liquid nitrogen supply
Aluminum foil and styrofoam dewar
liquid nitrogen level sensor
phase separator
reference in raised position
reference heater

Figure 1

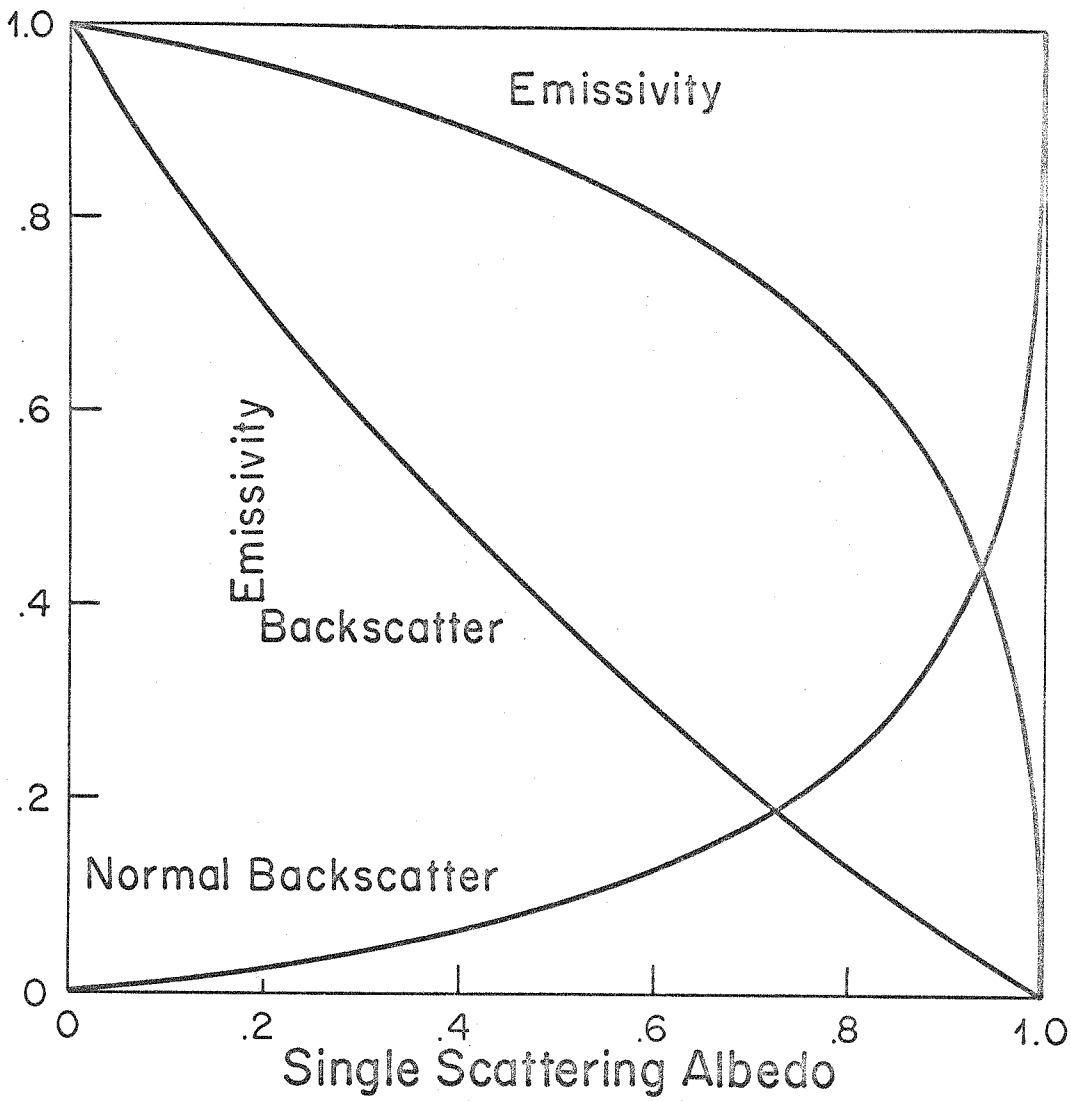

Figure 2. The theoretical relations between emissivity, normal backscatter, and single scattering albedo for a thick isotropic scattering medium. The theoretical maximum for normal backscatter is 1.057; here it is normalized to 1.0. The graph of emissivity (ordinate) versus normal backscatter (abcissa) shows that the emissivity is nearly equal to one minus the normal backscatter.

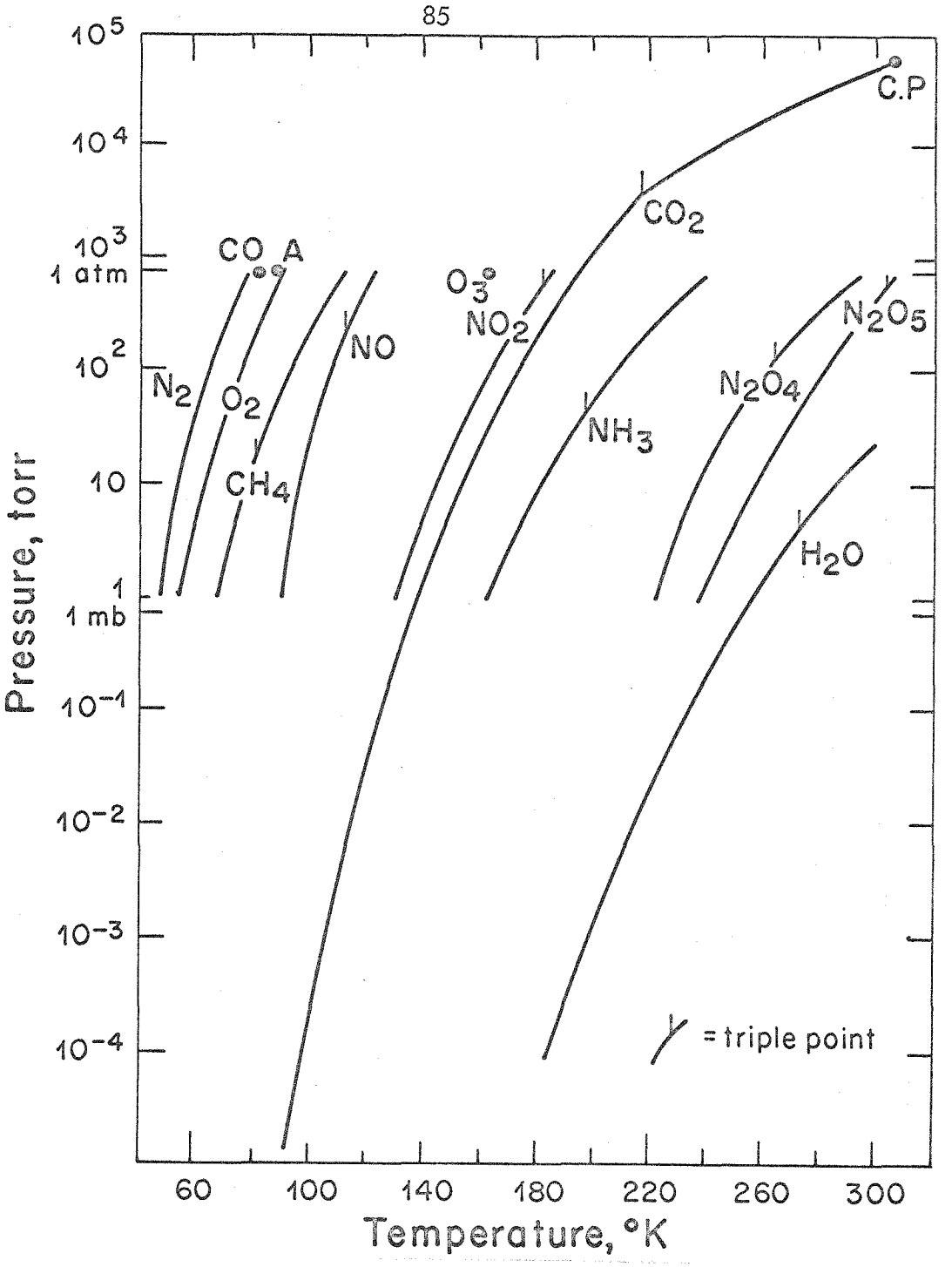

Figure 3. Saturation curves for CO_2, H_2O and several other gases.

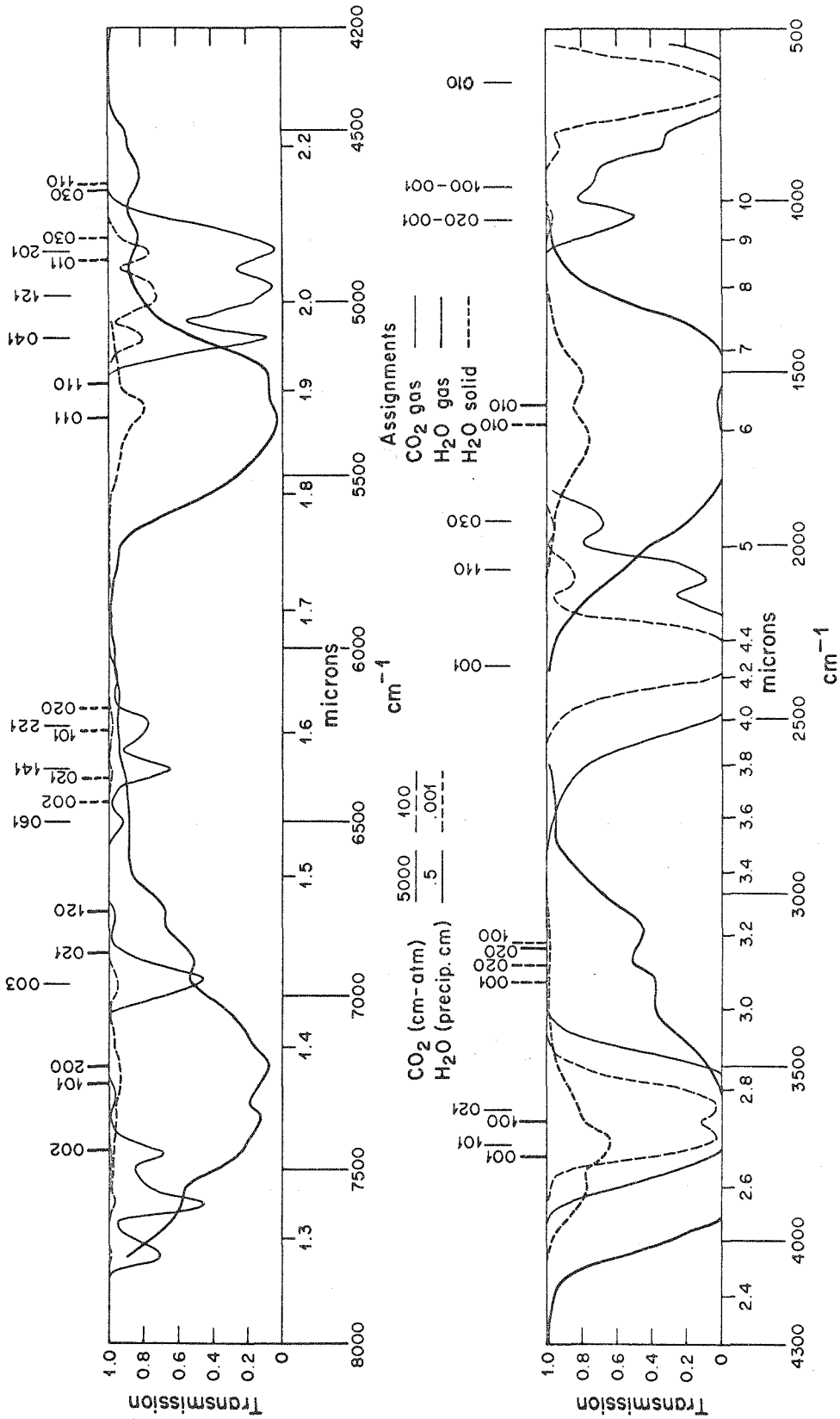
Transmission
1.0
0.8
0.6
0.4
0.2
0
8000
7500
7000
6500
6000
5500
5000
4500
4200
1.3
1.4
1.5
1.6
1.7
1.8
1.9
2.0
2.2
microns
cm⁻¹
002
104
200
003
021
120
061
002
021 141
101 221
020
041
121
011 201
030
030 410
Assignments
CO2 gas
H2O gas
H2O solid
020-001
100-001
010
030
110
001
CO2 (cm-atm) 5000 100
H2O (precip. cm) .5 .001
001
020
100
001
101
100 021
4300
4000
3500
3000
2500
2000
1500
1000
500
2.4
2.6
2.8
3.0
3.2
3.4
3.6
3.8
4.0
4.2 4.4
5
6
7
8
9
10
microns
cm⁻¹

Figure 4

APPENDIX FIGURE CAPTIONS

Figure 1. The chamber and spectral reflectometer. Drawn to scale, however most of the items have been rotated into this section. The auxilliary gas inlet, 12 watt lamp, inclined substage and mechanical feed-through, thermocouple pressure gauge, field lens heater, electrical feed-throughs and cooling coils and thermocouple sensors for baths other than liquid nitrogen are not shown.

Figure 4. Transmission spectra of CO_2 and H_2O gas. The data are from the calculations of Stull et al. (1964) and Wyatt et al. (1964) for 1 atmosphere pressure and 300°K temperature. The H_2O spectra correspond approximately to the amounts in the Martian atmosphere and terrestrial atmosphere during good dry conditions. The CO_2 spectra correspond approximately to the amounts in the Martian and terrestrial atmospheres. The H_2O solid bands involving stretching modes are shifted about 500 cm^{-1} from the vapor bands.

TABLE 1

Energy reaching the sample

Source	Flux milliwatt cm^{-2}
Constant sources	
Radiation from the chamber lid ($T=0^{\circ}C$, $\epsilon=.2$, 1 steradian)	1
Radiation from the chamber walls ($T=0^{\circ}C$, $\epsilon=1$, 5 steradian)	25
Conduction through the gas in the chamber (∇T= 8 deg cm^{-1}, K= 5×10^{-5} cal sec^{-1} cm^{-3} deg^{-1})	1.6
Typical values due to sample growth (CO_2 at 10^{-4} gm cm^{-2} sec^{-1})	
Cooling of the sample gas	15
Latent heat release	62
Convection by the gas in the chamber, estimated	15
Due to observations	
Maximum radiation from the monochrometer	.003
Visual observation lamp (12 watt)	2.4
Comparison rates	
Solar flux at the subsolar point on Mars	60
Blackbody radiation at	
$77^{\circ}K$ Liquid nitrogen	.2
$145^{\circ}K$ Martian CO_2 condensation	2.5
$190^{\circ}K$ Martian H_2O condensation	7.5
$300^{\circ}K$ Earth ambient	46

TABLE 2

Transmission data for the B and C filter sets.

Wavelength (μ)	Bandwidth (μ)	Peak Transmission (%)
	B Filter Set	
.8025	.0275	47
.850	.020	48
.900	.020	61
1.06	.010	51.5
1.10	.020	61
1.30	.020	58
1.40	.020	58
1.504	.020	57.5
	C Filter Set	
.793	.016	35.5
.843	.022	34
.890	.027	37
.949	.022	33
.997	.022	31.5
1.042	.020	27.5
1.092	.032	31
1.143	.042	40
1.194	.054	27.5
1.2425	.036	35
1.293	.040	29.5
1.343	.046	32
1.386	.065	32
1.445	.074	34
1.488	.056	27
1.547	.048	27
1.585	.068	32
1.646	.040	24

Table 3

Physical Properties of CO_2, H_2O and N_2
Data from I.C.T. and C.R.C.Handbook.

		Density gm cm^{-3} (gas x 10^3)		Specific Heat cal gm^{-1} $^oC.^{-1}$		Thermal Cond. cal cm^{-2} sec^{-1} $^oC.^{-1}$ cm^{-1} x 10^5		Latent Heat of Fusion (f) Vapor (v) Sublim.(s) Cal gm^{-1}	
		Value	T, $^oC.$	Value	T, $^oC.$	Value	T, $^oC.$	Value	T, $^oC.$
CO_2	Gas	1.977	STP	.20	15	3.28	0		
				.184	- 75	2.56	-50		
						2.18	-78		
	Liq.	.79	20	.492	0			55 v	0
		1.19	- 60	.442	- 50			88 v	- 60
	Sol.	1.53	20	.270	-100			43 v	- 56
		1.565	- 80	.215	-150			138 s	- 78
		1.627	-130	.160	-200				
H_2O	Gas	.805	STP	.482	100				
				.507	500				
	Liq.	1.000	0	1.0	0	140			
	Sol.	.917	0	.492	0	500		80 f	0
				.262	-140			596 v	0
				.156	-200				
N_2	Gas	1.251	STP	.247	15	5			
				.25	-100				
				.256	-181				
	Liq.	.81	-196					47 v	-196

REFERENCES

Alkezweeny, A. J., and P. V. Hobbs, The reflection spectrum of ice in the near infrared, J. Geophys. Res., 71, 1083-1086, 1966

Anderson, A., and S. H. Walmsley, Far infrared spectra of molecular crystals, 3. Carbon dioxide, nitrous oxide and carbonyl sulfide, Mol. Phys., 7 583-588, 1964.

Anderson, A., and H. A. Gebbie, Far infrared study of molecular crystals by interferometric methods, Spectrochimica Acta, 21, 883-888, 1965.

Bertie, J. E., and E. Whalley, Infrared spectra of ices Ih, and Ic in the range 4000-350 cm^{-1}, J. Chem. Phys., 40, 1637-1645, 1964.

Blau, H. H., Jr., R. P. Espinola, and E. C. Reifenstein, Near infrared scattering by sunlit terrestrial clouds, Applied Optics, 5, 555-564, 1966.

Burch, D. E., D. A. Gryvnak, and D. Williams, Total absorptance of carbon dioxide in the infrared, Applied Optics, 1, 759-765, 1962.

Capen, C.F., The Mars 1964-1965 Apparition, Jet Propulsion Lab. Tech. Report No. 32-990, 187 pp., 1966.

Caren, R. P., A. S. Gilcrest, C. A. Zierman, W. F. Schmidt, and J. P. Millard, Experimental and analytic investigation of the effect of cryo-deposits on the radiation properties of plain and extended surfaces, AEDC-TDR-63-270, 1963.

Chandrasekhar, S., Radiative Transfer, Dover, New York, 393 pp., 1960.

Cunningham, T. M., Jr., and R. L. Young, The radiative properties of carbon dioxide cryodeposits at 77°K, AEDC-TDR-62-165, 1962.

Cunningham, T. M., Jr., and R. L. Young, The absorptance of a water cryo-deposit at 77°K for 350°K radiation, AEDC-TDR-63-155, 1963.

Dawson, J. P., B. A. McCullough, B.E. Wood, and R. Birkebak, Thermal radiative properties of carbon cryodeposits, Sixth Annual Synposium on Space Environmental Simulation, McDonnelAircraft Corp., St. Louis, Missouri, 1965.

de Vaucouleurs, G., Physics of the Planet Mars, Faber and Faber, London, 365 pp., 1954.

Dollfus, A., Polarization studies of the planets, in Planets and Satellites, ed. G.P. Kuiper and B.M. Middlehurst, Univ. of Chicago, pp. 343-399, 1961.

Gierasch, P. and R. Goody, An Approximate Calculation of Radiative Heating and Radiative Equilibrium in the Martian Atmosphere, Planet. Space Sci., 15, 1465-1477, 1967.

Giguere, P.A., and K.B. Harvey, On the infrared absorption of water and heavy water in condensed states, Canadian J. Chem., 34, 798-808, 1956.

Goody, R.M., Atmospheric Radiation, Oxford, 463 pp., 1964.

Goody, R. and M.J.S. Belton, Radiative relaxation times for Mars, Planet. Space Sci., 15, 247-256, 1967.

Jacox, M.E., and D.E. Milligan, The infrared spectra of thick films of CO_2 and $CO_2 + H_2O$ at low temperatures, Spectrochimica Acta, 17, 1196-1202, 1961.

Kaplan, L.D., G. Münch, and H. Spinrad, An analysis of the spectrum of Mars, Astrophys. J., 139, 1-15, 1964.

Keegan, H.J., and V.R. Weidner, Infrared spectral reflectance of frost, J. Opt. Soc. Am., 523-524, 1966.

Kiess, C.C., S. Karrer, and H.K. Kiess, A new interpretation of Martian

phenomena, Publ. Astron. Soc. Pacific, 72, 256-267, 1960.

Kislovskii, L.D., Optical characteristics of water and ice in the infrared and radiowave regions of the spectrum, Optics and Spectroscopy (Soviet), VII, 201-206, 1959.

Kuiper, G.P., Planetary atmospheres and their origin, The atmospheres of the Earth and Planets, ed. G.P. Kuiper, Univ. of Chicago, pp. 306-405, 1952.

Leighton, R.B., and B.C. Murray, Behavior of Carbon dioxide and other volatiles on Mars, Science, 153, 136-144, 1966.

Leovy, C., Mars ice caps, Science, 154, 1178-1179, 1966.

Lippincott, E.R., R.V. Eck, M.O. Dayhoff, and C. Sagan, Thermodynamic equilibria in planetary atmospheres, Astrophys. J., 147, 753-764, 1967.

Marshall, J.V., An improved test for NO_2 on Mars, Comm. Lunar and Planetary Lab., 2, 167, 1964.

Mason, B.J., The Physics of Clouds, Oxford, 481 pp., 1957.

McDonald, R.K., and R.W. Deltenre, Cirrus infrared reflection measurements, J. Optic. Soc. Amer., 53, 860-868, 1963.

McSwain, B., and J. Bernstein, Physical Properties of Water: Specular Reflectance of Water in the 1.5 to 15-micron Region as a Function of Wavelength and Incidence Angle, NAVWEPS 7162 (NOLC 539) Part 1, Foundation Research Proj., Quart. Rep., 1961.

Moroz, V.I., On the infrared spectra of Jupiter and Saturn ($0.9 - 2.5\ \mu$), Soviet Astronomy-AJ, 5, 827-830, 1962.

Moroz, V.I., The infrared spectrum of Mars (λ 1.1 - 4.1 μ), Soviet Astronomy-AJ, 8, 273-281, 1964.

Ockman, N., The infrared and raman spectra of ice, Advan. Phys., 7, 199-220, 1958.

Osberg, W.E., and D.F. Hornig, The vibrational spectra of molecules and complex ions in crystals, VI. Carbon dioxide., J. Chem. Phys., 20, 1345-1347, 1952.

Owen, T., The composition and surface pressure of the Martian atmosphere: results from the 1965 opposition, Astrophys. J., 146, 257-270, 1966.

Ron, A., and O. Schnepp, The lattice vibrations of the solids N_2, CO_2 and CO, J. Chem. Phys., 46, 3991-3998, 1967.

Schorn, R.A., H. Spinrad, R.C. Moore, H.J. Smith, and L.P. Giver, High-dispersion spectroscopic observations of Mars, II. The water-vapor variations, Astrophys. J., 147, 743-752, 1967.

Spinrad, H., R.A. Schorn, R. Moore, L.P. Giver, and H.J. Smith, High-dispersion spectroscopic observations of Mars, I. The CO_2 content and surface pressure, Astrophys. J., 146, 331-338, 1967.

Stull, V.R., P.J. Wyatt, and G.N. Plass, The infrared absorption of Carbon Dioxide, Infrared transmission studies, Vol. III, Rept. SSD-TDR-62-127, Space Systems Division, Air Force Systems Command, Los Angeles, 1963.

Stull, V.R., P.J. Wyatt, and G.N. Plass, The infrared transmittance of carbon dioxide, Applied Optics, 3, 243-254, 1964.

White, H.F., The vibrational spectrum and structure of ice at low temperature, Thesis, Brown University, Dept. of Chem., 1952.

Wood, B.E., A.M. Smith, and B.A. McCullough, The spectral reflectance of water and carbon dioxide cryodeposits from 0.36 to 1.15 microns, AEDC-TR-67-131.

Wyatt, P.J., V.R. Stull, and G.N. Plass, The infrared transmittance of water

vapor, Applied Optics, 3, 229-241, 1964.

Zander, R., Spectral scattering properties of ice clouds and hoarfrost, J. Geophys. Res., 71, 375-378, 1966.

Zimmerman, R., and G.C. Pimentel, The infrared spectrum of ice: Temperature dependence of the hydrogen bond potential function, Adv. in Molecular Spectroscopy, 2, 726-737, 1962.